Diploma Thesis

Dental Biometrics: Human Identification Based On Dental Work Information

In accordance with the
Carinthia University of Applied Sciences

In cooperation with the
Universidade Estadual Paulista, Bauru, Brazil

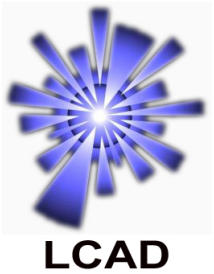

School of
Medical Information Technology

Laboratory of
High Performance Computing
Department of Computer Science

supervised by
DI Dr. Pierre Elbischger

and supervised by
Dr. Aparecido Nilceu Marana

submitted by

Michael Hofer

Matriculation number: 0310099032

Klagenfurt, June 2007

To Ines, who always stands behind me and
lets me go my ways when I have to.

***

To my family, who always supports me
wherever and whenever they can.

***

To my philosophy teachers
Dr. Patricia Winkler-Payer and Dr. Wigbert Winkler,
who introduced me to Philosophy and its deeper meanings.

Thank you

The most beautiful thing
we can experience is the mysterious.
It is the source of all true art and science.

Albert Einstein

Abstract

Dental biometrics is used in the forensic odontology to identify individuals based on their dental characteristics. Unlabeled post-mortem dental radiographs are compared with labeled ante-mortem dental radiographs stored in a database to find the highest similarity. This work presents a method for human identification based on dental work information extracted out of panoramic dental radiographs. The proposed method consists of three main processing stages: (i) feature extraction, (ii) creation of a dental code and (iii) matching. In the first stage, seed points of the dental works are detected by thresholding. A refined segmentation is obtained by using a snake (active contour) algorithm. The dental code incorporates information about the position (upper or lower jaw) and size of the dental works, and the distance between neighboring dental works. The matching stage is performed with the Levenshtein distance (Edit distance) which is used to infer the subject's identity. The costs of the insertion, deletion and substitution operations, which are needed to calculate the Levenshtein distance, were tuned to make the matching algorithm more sensitive. The method was tested on a database including 68 dental radiographs and the results are encouraging. An equal error rate (EER) of 9.8% using ROC analysis and an accuracy of 82% for top-1 retrieval were achieved.

Keywords: dental biometrics, biometrics, forensic odontology, dental radiograph, snake, Levenshtein distance.

Kurzfassung

Dental Biometrie wird in der forensischen Zahnmedizin zur Identifikation von Personen basierend auf deren Dentalcharakteristika eingesetzt. Dabei werden ungekennzeichnete Dentalröntgenbilder mit gekennzeichneten Dentalröntgenbildern, gespeichert in einer Datenbank, verglichen um die größte Übereinstimmung zu finden. In dieser Arbeit wird eine Methode zur Identifizierung von Personen vorgestellt, welche auf Informationen der Dentalarbeiten basiert. Die benötigten Informationen werden aus Panorama-Dentalröntgenbildern extrahiert. Die vorgestellte Methode beinhaltet drei Verarbeitungsstufen: (i) Merkmalextrahierung, (ii) Erstellen eines Dental Codes und (iii) vergleichen von Dental Codes (matching). In der ersten Stufe werden die Dentalarbeiten durch Thresholding detektiert. Das Segmentierungsergebnis wird mit Hilfe eines Snakes (aktive Konturen) Algorithmus verfeinert. Der Dental Code wird aus Informationen wie der Position (Ober- oder Unterkiefer) und Größe der Dentalarbeiten, sowie der Distanz zwischen zwei benachbarten Dentalarbeiten erstellt. Die Matching-Stufe verwendet die Levenshtein Distanz (Edit Distanz) um die Identität der zu prüfenden Person zu bestimmen. Die Kosten für die Operationen Einfügen, Löschen, und Ersetzen, welche für die Berechnung der Levenshtein Distanz benötigt werden, wurden adaptiert um die Matching-Ergebnisse zu verbessern. Die Methode wurde an einer Datenbank mit 68 Dentalröntgenbildern getestet wobei viel versprechende Ergebnisse erzielt wurden. Eine Gleichfehlerrate (EER) von 9.8% wurde bei der Verwendung einer ROC Analyse ereicht. 82% aller Personen konnten durch das Matching-Ergebniss an erster Stelle wieder erkannt werden.

Suchbegriffe: Dental-Biometrie, Biometrie, forensische Zahnmedizin, Dentalröntgenbild, snake, Levenshtein Distanz.

Contents

List of Figures

List of Tables

Chapter 1

Introduction

The field of biometrics has received much attention in the last years because it is an interesting alternative to traditional authentication systems like passwords. Under severe circumstances, e.g. encountered in mass disasters, conventional biometric characteristics, such as fingerprints, may not be able to be used because of their low resistance. In such cases, dental features are considered the best candidates for the process of identification. The objective of forensic odontology (forensic dentistry) is it to identify individuals based on their dental characteristics. To achieve this aim, dental biometrics automatically analyzes dental radiographs through comparing unlabeled post-mortem (PM) radiographs, acquired after death, with labeled ante-mortem (AM) radiographs, acquired before death, and stored in a database.

In this work a new dental biometric identification method based on information of dental works (dental restorations) is introduced. The proposed method consists of three main stages, see Fig. 1.1: (i) feature extraction, (ii) generation of a dental code and (iii) feature matching. During the feature extraction stage, information of the dental works, such as size and relative location to other dental works, are extracted. In stage two, a dental code is created out of this information and is matched, in stage three, against stored dental codes in a database.

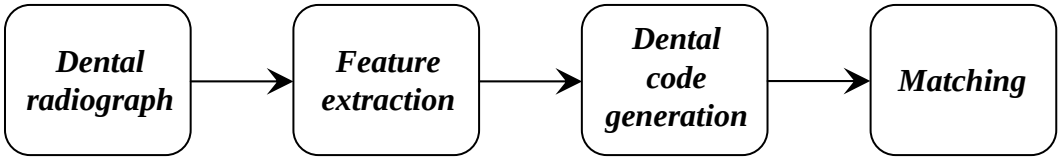

Figure 1.1: Block diagram of the newly proposed dental biometric identification method based on information of dental works (dental restorations).

The diploma thesis is organized as follows. Chapter two gives an overview about the topic biometrics. Detailed information about dental biometrics and forensic odontology is given in chapter three. Chapter four describes the image processing methods and algorithms like snakes (active contours) and the Levenshtein distance that were used in the presented work. The proposed biometric method based on dental works information is described in chapter five, followed by the results and a discussion sections in the chapters six and seven.

1.1 Motivation

Based on the information provided by experts from the Criminal Justice Information Services Division (CJIS) of the FBI, there are over 100,000 unsolved cases of missing persons in the National Crime Information Center at any given point in time. 60 percent of these cases have remained in the computer system for 90 days or longer [1]. Dental records also have been used to identify the victims of disasters, such as the 9/11 terrorist attack and the Asian tsunami [2, 3]; thus the importance of using dental records for human identification is now well recognized. According to these facts, there are two main advantages to automate the procedure of dental identification. First, an automatic process will be able to compare the post-mortem(PM) records against ante-mortem (AM) records to determine the closest match of multiple identities and second, an automatic (or semi-automatic) system can perform identification utilizing a large database while a manual (or non-automated) system is only useful for verification on a small data set [4].

Chapter 2

Biometrics - Overview

The following chapter provides an overview of the topic biometrics. Basic biometric terms and the process of a biometric system are described and an introduction to common biometric modalities is given. Finally, performance testing methods for biometric systems are shown including the receiver operating characteristics (ROC) curve analysis.

2.1 Introduction

The field of biometrics has received much attention in the last years because it is an interesting alternative to traditional authentication systems such as passwords, personal identification numbers (PINs) or smartcards which are dependent on individually-related information.

The origin of the term *biometrics* is derived from the Greek words *bio* for *life* and *metron* for *to measure*, and is used to describe a characteristic or a process. As a characteristic it means a measurable anatomical, physiological and/or behavioral characteristic. As a process it means an automated method of recognizing individuals through their biometric characteristics [5].

2.1.1 History of Biometrics

The history of biometric methods goes back thousands of years, e.g., 500 B.C. in Babylon where fingerprints were recorded in clay tablets to be used as a person's mark for business transactions [5]. In scientific literature human identification using body measurements dates back to the 1870's when Alphonse Bertillon proposed a body measurement system including measures like skull diameter, arm and foot lengths. The system was used until the 1920's to identify prisoners in the USA. Quantitative identification through fingerprint and facial measurements was first proposed by Henry Faulds, William Herschel and Sir Francis Galton Herschel in the 1880's. The development of true biometric systems began

to start in the second half of the 20th century coinciding to the development of new signal processing techniques. In the 1960's fingerprint and speaker recognition systems were researched followed by the development of hand geometry systems in the 1970's. Retinal, signature verification and face systems came up in the 1980's. In the 1990's the first iris recognition algorithm was patented and iris recognition became available as a commercial product. Biometric systems began to emerge in everyday applications in the early 2000's [5, 6].

2.1.2 Classification of Biometric Characteristics

A biometric characteristic can be described with five qualities [6]:

1. **Robustness:** The biometric characteristic should be stable and not change over time.
2. **Distinctiveness:** To clearly recognize an individual, the biometric characteristic should show great variation over the population.
3. **Availability:** The entire population should ideally have the measured biometric characteristic.
4. **Accessibility:** The biometric characteristic should be easily acquired using electronic sensors.
5. **Acceptability:** The process of acquiring biometric measurement should be easy and user friendly which means that people do not object to having this measurement taken.

Biometric systems can be divided into *behavioral* and *physical (physiological)* systems:

Behavioral biometric

Behavioral biometrics are characterized by a behavioral trait that is learnt and acquired over time [7]. It is the reflection of an individual's psychology. Behavioral characteristics can change over time which means that a behavioral biometric system needs to be designed more dynamically and accept some degree of variability [8]. Physiological elements may influence the monitored behavior in specific behavioral biometric techniques, e.g. keystroke dynamics, signature verification and speaker verification [7].

Physical (physiological) biometric

Physical biometrics are characterized by a physical characteristic rather than a behavioral trait, e.g. fingerprint, face or the blood vessel pattern in the hand [8]. It does not change over time which means it is more stable than a behavioral biometric. Behavioral elements may influence the biometric sample captured [7], e.g. tremor during a fingerprint acquisition.

2.1.3 Identification vs. Verification

Verification (verify) is defined by the process of matching (comparing) a given biometric data (not stored in a database) with the biometric reference template (stored in a database) of a single person (enrolee) whose identity is being checked to determine whether it matches the enrolee's template [7]. Verification systems are used, e.g. to access control to high security areas.

Identification (identify) is defined by the one-to-many process of matching submitted biometric data against all other biometric reference templates to determine whether it matches any of the templates and to determine the identity of the enrolee whose template matches the biometric data [7]. Identification systems are used, e.g. to determine the identity of the person, whose fingerprints have been found at a crime scene.

2.2 The Biometric Process

The biometric process is divided into five main stages, see Fig. 2.1:

1. **Data collection:** Capturing a biometric sample (raw data of a biometric characteristic before pre-processing) from a claimant, who wants to proof his/her identity. If there is no reference template in the database, the person must first register the biometric characteristic (e.g. a fingerprint) to be included into the database. This process is called enrollment. If the person is already enrolled, the process is called authentication (verification or identification) which means establishing confidence in the truth of the determination [5].

2. **Feature extraction:** After the pre-processing of the biometric sample, an algorithm extracts the unique features derived from the biometric sample and converts it into biometric data so that it can be matched to a reference template in the database [7].

3. **Template database:** In the case of enrolment biometric data are stored in a template database. In the case of authentication, biometric data are matched against a reference template from the template database.

4. **Matching:** In the matching stage, biometric data are matched (compared) with data contained in one (verification) or more (identification) reference template(s) to score a level of similarity.

5. **Deciding:** The acceptance or rejection of biometric data is dependent on the scored level of similarity in the matching stage, falling above or below a defined threshold. The threshold is adjustable so that the biometric system can be more or less strict, depending on the requirements of any given biometric application [7].

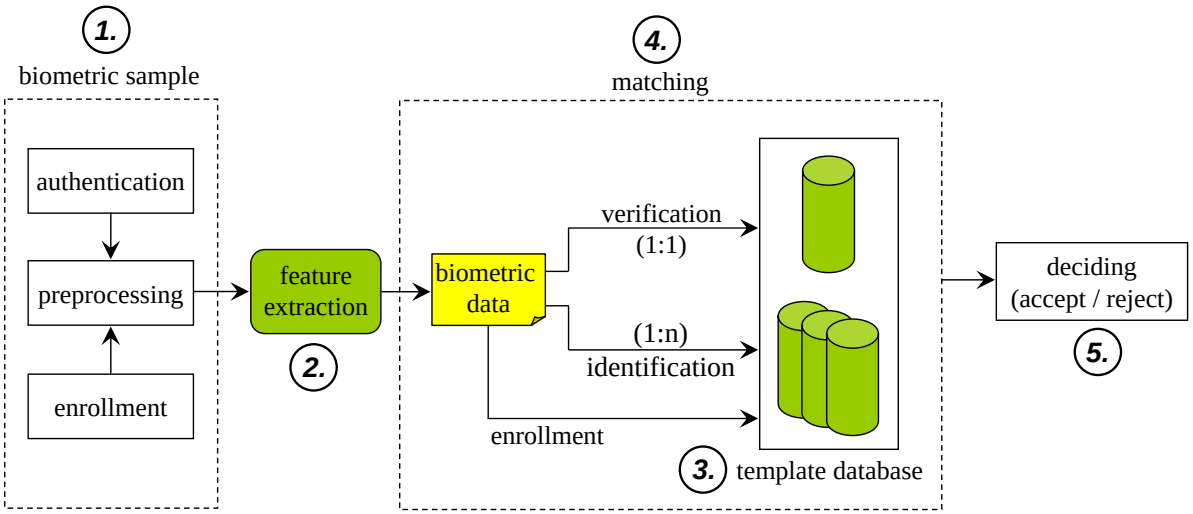

Figure 2.1: Model of the biometric process: 1. Capturing of the biometric sample; 2: The biometric sample is converted into biometric data by extracting its unique features; 3: The reference templates are scored in the template database; 4: Matching of the biometric data with one or more reference template(s); 5: Acceptation or rejection of the claimant.

2.3 Biometric Modalities

Many biometric modalities are in various stages of development and are used to secure areas, maintain time records and to enhance user convenience. Presently, no modality can be said to be the best for all implementations. When implementing a biometric system, various factors have to be discussed: factors such as location, number of users, user circumstances (e.g. disabilities), already existing data which can be used (e.g. already existing fingerprint images), etc. [5, 9]. To improve the performance of biometric systems, different biometric modalities can be combined to multibiometric systems (or multimodal biometric systems) [10]. Commonly studied and implemented biometric modalities include face, iris, fingerprint and hand geometry recognition.

2.3.1 Face Recognition

Face recognition is a physical biometric that analyzes the characteristics of a person's face. The data collection is performed through a digital video camera. The face recognition problem can be solved with two different approaches: geometric (feature based) and photometric (appearance based) [5]. A major advantage of face recognition is that it is contactless, which, however, can also be a drawback for the user acceptance. Another problem is that face recognition systems are not very resistant against fraud because it is difficult for them to decide, if the captured image is a real person or only a picture. They are used for identification, e.g. at airports, but also for verification, e.g. to verify passport images at frontiers and border crossings [9].

2.3.2 Iris Recognition

The iris is a muscle within the eye which regulates the size of the pupil to control the amount of light that enters the eye. Iris recognition is a physical biometric that recognizes a person by analyzing the person's iris. Features, which are found in the colored ring of tissue surrounding the pupil, are extracted and matched [5, 7]. Therefore, an IrisCode® [11] is created out of more than 200 points including rings, furrows and freckles, which can be used for the comparison, see Fig. 2.2[1].

Even the left and right eye of the same person are unique from one another which makes iris recognition very powerful for identification and verification purposes. The iris is also stable over time and can be easily imaged. A drawback of the system is that people often do not have the willingness to hold their eyes into the spot of the scan. Iris recognition systems are used, e.g. in jails as a security check for employees and at airports to allow frequent passengers to streamline boarding procedures [6].

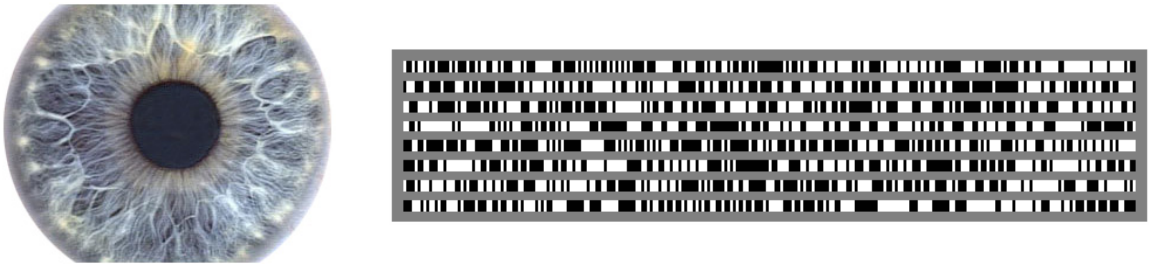

Figure 2.2: An iris recognition system uses an (a) iris image to create an IrisCode®. The IrisCode® is a biometric feature format used in the Daugman iris recognition system. (b) Pictorial representation of an IrisCode®: A 2D Gabor wavelet filters the segments of the iris image into phasors (vectors). These phasors include information on the orientation and spatial frequency and the position of these areas. This information is used to map the IrisCode® [5].

2.3.3 Fingerprint Recognition

Fingerprint recognition is a physical biometric that uses the physical structure of an individual's fingerprint for recognition purposes. The features which are used in fingerprint recognitions systems are extracted out of minutiae points (e.g. ridge bifurcations and ridge endings), see Fig. 2.3[2]. The matching algorithm maps the minutiae points in relative placement on the finger and searches through a database for similar minutia information. In some methods only the set of data that is used for comparison and not the image of the fingerprint is stored in the database to alleviate the public's fear. Some systems also measure the blood flow of the fingers to prevent the abuse of fake fingers.

[1] Source: John Daugman, University of Cambridge; *http://www.cl.cam.ac.uk/~jgd1000/sampleiris.jpg*
[2] Source: Department of Electrical and Computer Engineering, University of Delaware; *http://www.ee.udel.edu/~barner/courses/eleg675/Images/Fingerprint.jpg*

Fingerprint recognition systems are used, e.g., to secure entry devices for building door locks, computer network access and criminal investigations [6, 11].

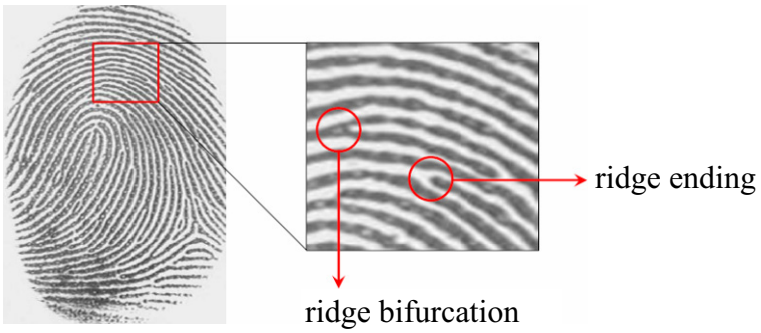

Figure 2.3: Minutia points of a fingerprint (ridge bifurcations and ridge ending).

2.3.4 Hand Geometry Recognition

Hand geometry recognition is a physical biometric that uses the concept of analyzing the physical structure of an individual's hand. A camera captures the top surface and a side image of the hand. The measurements range from the length of the fingers, the distance between knuckles, to the height or thickness of the hand and fingers [5, 11], see Fig. 2.4[3]. The systems are very user friendly and can be easily integrated into other devices or systems because no special hardware is needed. A drawback of the system is that the human hand is not unique, like a fingerprint. Therefore, it is mostly used for verification of a known biometric reference template database. Hand geometry recognition is widely used for applications in physical access and personal verification [5, 6].

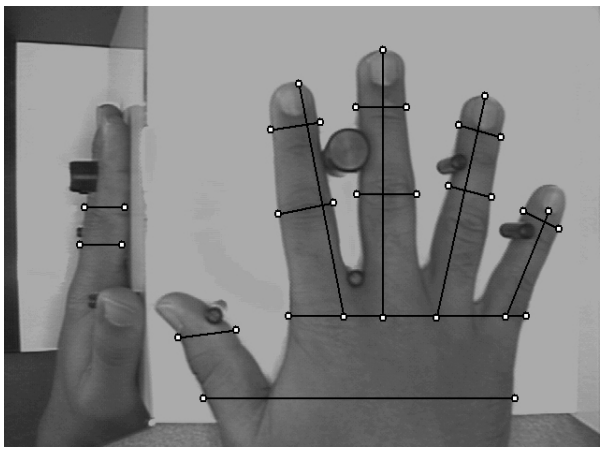

Figure 2.4: Captured image of a hand including example distance measurements.

[3] Source: Biometrics Research, Michigan State University; *http://biometrics.cse.msu.edu/hand_geometry.html*

2.3.5 Other Biometric Identification Modalities

Biometric identification modalities can be divided into physical and behavioral biometrics. A clear border between these two kinds of biometrics cannot be made, because physiological elements may influence the monitored behavior in specific behavioral biometric techniques (e.g. signature verification) and vice versa. In the following, biometric identification modalities are categorized whether if they are more like physical or behavioral biometrics.

Physical Biometrics

- **Retina recognition** analyzes the unique pattern of blood vessels situated at the back of the eye [7]. For the acquisition of the image of the retina, near infrared light is produced using light emitting diodes (LEDs) [5].
- **Vascular/Vein pattern recognition** analyzes the vein patterns of a hand or a finger. Near infrared light is used to capture images of blood vessels. Features such as vessel branching points, vessel thickness, and branching angles are extracted and analyzed [7].
- **Facial thermography** senses heat in the face, caused by the flow of blood under the skin [7].
- **Ear biometric** analyzes mainly two features: The shape of the ear (ear geometry) and/or thermogram pictures of the ear. The ear structure is quite complex, but it is still being discussed by researchers if it is unique for all individuals [12].
- **Palm print recognition** analyses the aggregate information presented in a friction ridge impression of a palm. This information includes the flow of the friction ridges, the presence or absence of features along the individual friction ridge paths and their sequences, and the intricate detail of a single ridge [5].
- **DNA biometric:** Deoxyribonucleic acid (DNA) is a molecule that encodes genetic information. DNA biometrics differs from standard biometrics in several ways: (i) DNA requires a tangible physical sample, (ii) the matching is not done in real-time, (iii) not all stages of comparison are automated, (iv) DNA matching does not employ templates or feature extraction, but rather represents the comparison of actual samples. Regardless of these basic differences, DNA is a type of biometric inasmuch as it is the use of a physical characteristic to verify or determine identity [13].

Behavioral Biometrics

- **Speaker/Voice recognition** analyzes the pattern in speech of the individual. Speech is influenced by the physical structure of an individual's vocal tract and behavioral characteristics [11].
- **Dynamic signature** analyzes the way an individual signs his/her name. Signing features such as speed, velocity and pressure exerted by a hand holding a pen are used as well as the static shape of the finished signature [7].
- **Keystroke dynamics** analyzes the typing rhythm of an individual typing onto a keyboard [7].
- **Gait/Body recognition** recognizes people according to their walking patterns including parameters such as step length, step width, walking speed and joint rotation of the hip, knee and ankle [14].

2.4 Biometrics: Privacy's friend or foe?

Biometrics is a relatively new technology, which is being deployed in public and private sector applications. As this technology becomes more economical and technically perfected, and it will become even more commonplace, the field of biometrics have to deal with legal and policy concerns. Critics inevitably compare biometrics to Big Brother and the loss of individual privacy. On the other hand, people using biometrics stress the greater security and improved service that the technology provides. These facts lead to the question whether biometrics is privacy's friend or privacy's foe [15]?

Before addressing the criticisms of biometrics as privacy's foe, the counter case needs to be made: biometrics is privacy's friend. Critics of biometrics are too quick to kill the biometric identifier when it is really the "information society" and the technical support of computer matching that should be the focus of their concern. Biometrics protects information integrity in both the private and public sectors. By restricting access to personal information and by allowing maximum choice for the organization, biometrics provides effective privacy protection [15]. In my opinion, biometrics is a technological reality that promises greater security and efficiency for both its public and private sector users, which indicates that biometrics is more privacy's friend than privacy's foe.

2.5 Biometric Performance Testing and Statistic

The accuracy of a biometric system is determined through a series of tests. A complete evaluation of a system for a specific purpose is divided into three main stages before a biometric system can be used and the full operation begins [16]:

1. **Technology evaluation**, where the accuracy of the matching algorithm is assessed.
2. **Scenario evaluation**, where the performance of the matching algorithm in a mock environment is tested.
3. **Operational evaluation**, where the biometric system is finally tested live on site.

2.5.1 Performance Testing Methods

To measure the performance of a biometric system, statistics are used:

False acceptance rate (FAR)

The FAR is the percentage of times, a system produces a false accept, which occurs when a person is incorrectly matched to another person's existing biometric. Its value is one, if all impostor templates (templates of different persons) are falsely accepted and zero, if no impostor template is accepted. The FAR is similar to the false match rate (FMR) [11].

False rejection rate (FRR)

The FRR is the percentage of times, a system produces a false reject, which occurs when a person is not matched to his/her own existing biometric template. Its value is one, if all genuine templates (templates of the same person) are falsely rejected and zero, if no genuine template is rejected. The FRR is similar to the false non-match rate (FNMR), except the FRR includes the failure to acquire (FTA) rate and the FNMR does not. The FTA is the failure of a biometric system to capture and/or extract usable information from a biometric sample [11].

The five qualities of a biometric characteristic (see chapter 2.1.2) are quantified by the following measures [6]:

1. The **robustness** is measured by the FRR and is the percentage that the matching of a submitted biometric sample with an enrolled genuine template fails.
2. The **distinctiveness** is measured by the FAR and is the percentage that a submitted biometric sample matches with an enrolled impostor template.

3. The **availability** is measured by the failure to enroll (FTE). The FTE is the proportion of the population of claimants, failing to complete enrollment [7]. Common failures include end users who are not properly trained to provide their biometrics, the sensor not capturing information correctly, or captured sensor data of insufficient quality to develop a template [11].

4. The **accessibility** can be quantified by the throughput rate. The throughput rate is the number of claimants that a biometric system can process within a certain time interval [7].

5. The **acceptability** is measured by interviewing the claimants and analyzing the obtained results.

Out of the mentioned testing methods it cannot be said which biometric characteristic is the best. Their importance is highly dependent on the specific applications, the population and the used hardware/software system.

2.5.2 Performance Testing using ROC Analysis

The received metrics of the robustness and the distinctiveness (see chapter 2.5.1) are complexly correlated to each other but can be manipulated by using administration methods like thresholding.

Thresholding (False Acceptance / False Rejection)

To compare two biometric templates, a matching score is calculated which represents their similarity. The higher the score, the higher is the similarity between them. The genuine scores (matching scores of genuine templates) should always be higher than the impostor scores (matching scores of impostor templates), which is normally not possible in real world biometric systems. A decision made by a biometric system is either a genuine type of decision or an impostor type of decision, which can be represented by two statistical distributions called genuine distribution and impostor distribution, see Fig. 2.5. For each type of decision there are two possible decision outcomes: true or false. Therefore, there are a total of four possible outcomes: (i) a genuine individual is accepted, (ii) a genuine individual is rejected, (iii) an impostor is rejected, and (iv) and impostor is accepted. Outcomes (i) and (iii) are correct whereas (ii) and (iv) are incorrect. To separate the two distributions, a classification threshold is chosen which leads to some classification errors [6].

The FAR, the FRR and the equal error rate (ERR) are used to indicate the identification accuracy of a biometric system, see Fig. 2.5. The EER is defined as the point where the FAR and FRR intersect and have the same value, see Fig. 2.6. The EER of a system can be used to give a threshold independent performance measure. The lower the EER the better is the performance of the biometric system [6].

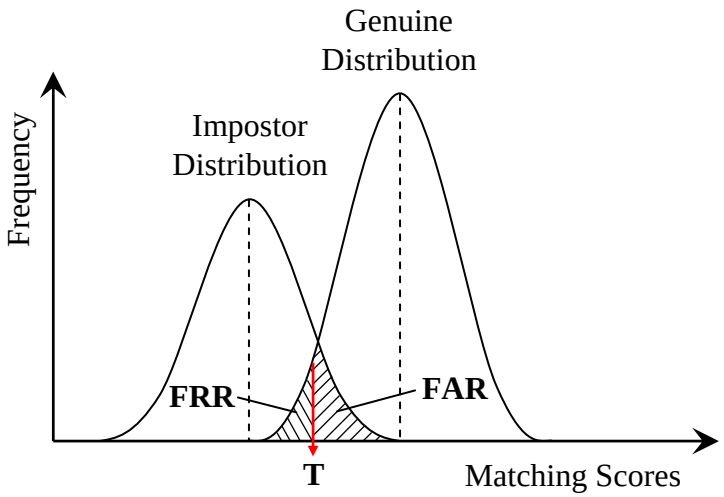

Figure 2.5: Score distributions for the impostor and genuine matching scores of a simulated biometric system. Given a matching score threshold (T), the area below T under the genuine distribution represents the FRR. The area above T under the impostor distribution represents the FAR.

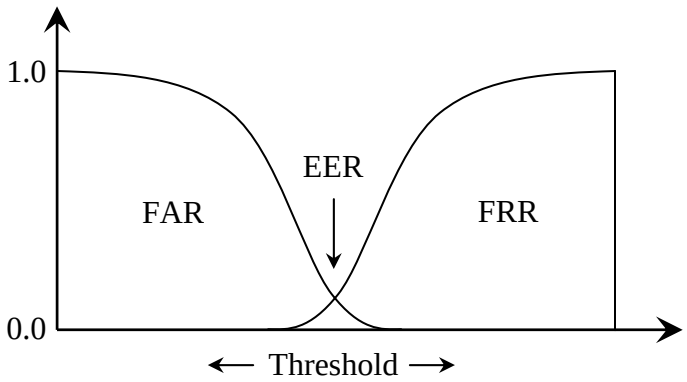

Figure 2.6: Values of the FAR and the FRR for a varying threshold for the score distributions in Fig. 2.5

Receiver Operating Characteristic (ROC) Curve

A Receiver Operating Characteristic (ROC) curve of a system illustrates the FRR and FAR for all thresholds. Each point on the ROC defines FRR and FAR for a particular threshold. High security access applications are concerned about break-ins and, hence, operate with a threshold at a point on ROC with small FAR. Forensic applications desire to catch a criminal even at the expense of examining a large number of false accepts and, hence, operate with a threshold at a high FAR. Civilian applications attempt to operate at operating points with both low FRR and low FAR, see Fig. 2.7 [6].

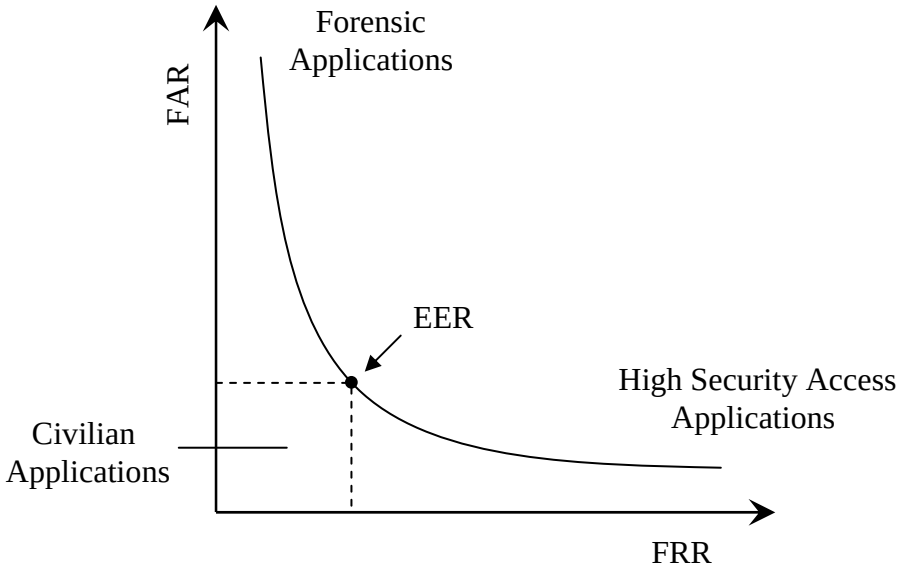

Figure 2.7: Receiver operating characteristic (ROC) curve. The point on the ROC curve where the FAR is equal to the FRR is represented by the EER.

2.5.3 Creation of the ROC Curve

To create the ROC curve of a biometric system, the genuine scores (matching scores of genuine templates) and the impostor scores (matching scores of impostor templates) are calculated and normalized in a way that the sum of all genuine scores and the sum of all impostor scores is one, see Fig. 2.8. To achieve the distributions for the genuine and impostor matching scores, the scores are commutatively summed up, see Fig. 2.9.

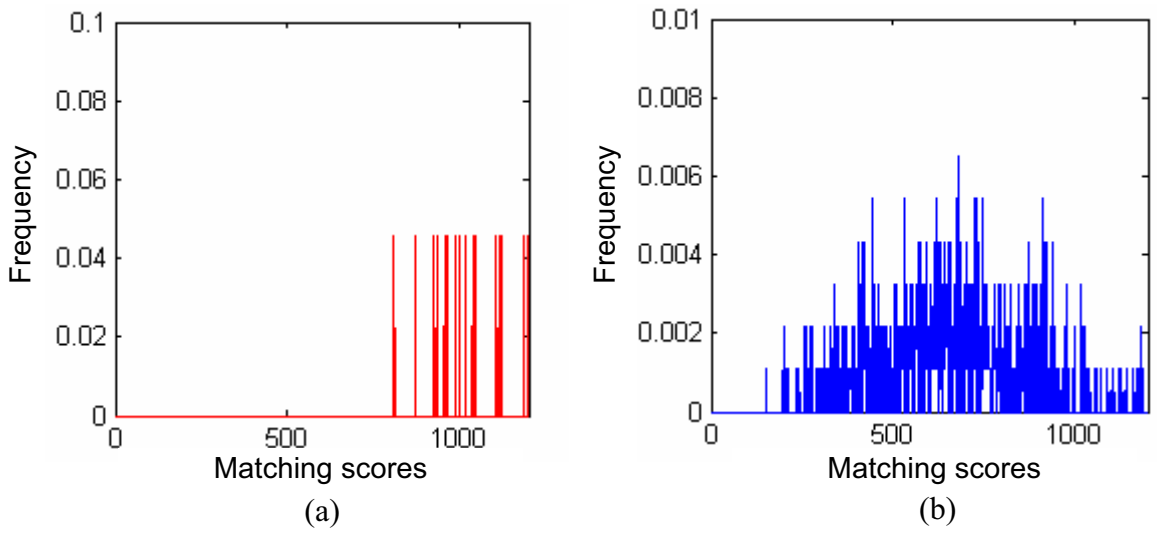

Figure 2.8: Matching scores for (a) genuine and (b) impostor templates.

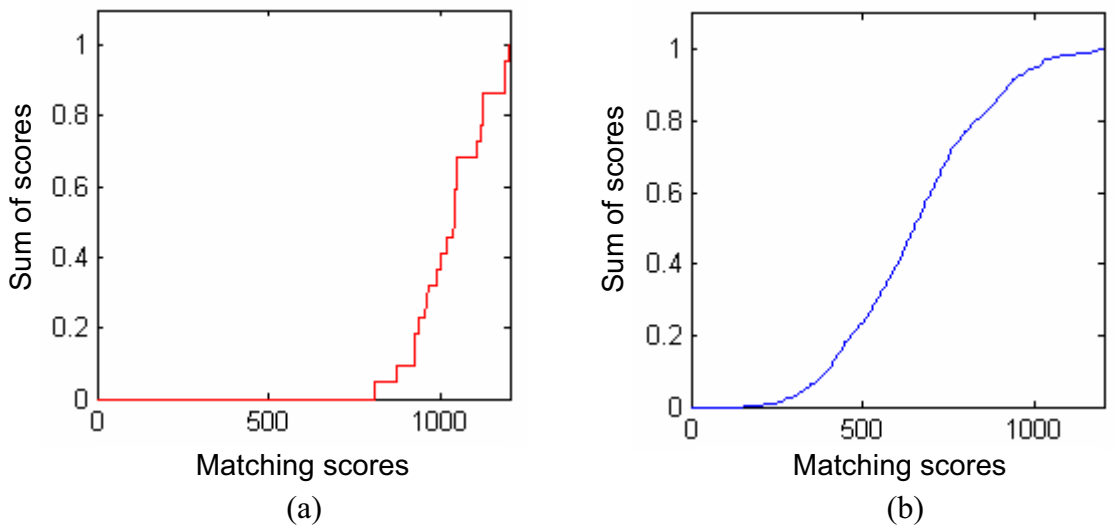

Figure 2.9: Distributions for (a) genuine and (b) impostor matching scores.

Finally, both distributions are displayed in one diagram. The complement of the impostor score distribution is calculated to visualize the threshold at the EER, see Fig. 2.10(a). The ROC curve illustrates the FRR and the FAR for all thresholds in one diagram, see Fig. 2.10(b).

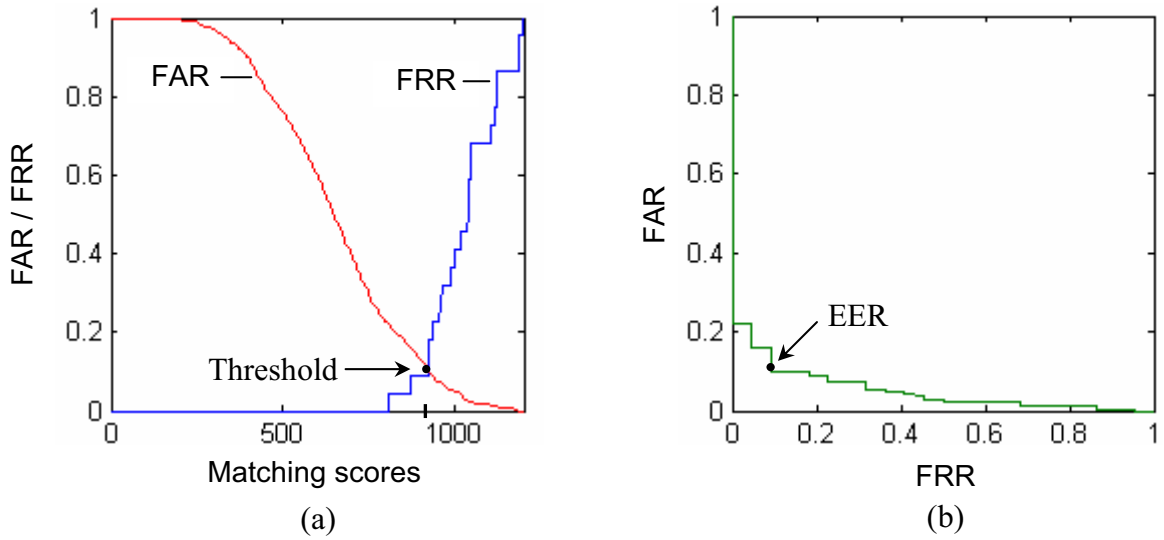

Figure 2.10: ROC curve. (a) Genuine and impostor distribution in one diagram to visualize the threshold at the EER (Threshold=908). (b) The FAR versus the FRR in one diagram (EER=10.6%).

2.5.4 Comparison of Biometric Systems

Two or more biometric systems cannot be compared if just one of the values FARs or FRRs are given. Both parameters have to be provided to compare the systems because in some cases, it is possible that the system with the lower FAR has an unacceptable high FRR and vice versa.

The values FAR and FRR are dependent on the selected threshold. As mentioned in chapter 2.5.1, the EER can be used to give a threshold independent performance measure. Another method for a comparison is to calculate the area under the ROC curve (AUC).

Finally, to compare the results of two or more biometric systems, it is necessary that the compared EERs or AUCs values are calculated on the same test data using the same test conditions, e.g. the same test protocol [6, 17].

Chapter 3

Dental Biometrics

The following chapter gives an overview of the topic dental biometrics which is used in forensic identification. The field of forensic odontology is explained and information about teeth as biometric characteristics is given. Finally, related works in the field of dental biometrics are presented.

3.1 Introduction

Law enforcement agencies have been exploiting biometric identifiers for decades as key tools in forensic identification. A huge volume of cases, which needs to be investigated by forensic specialists, leads to an automation of forensic identification.

Dental biometrics automatically analyzes dental radiographs to identify deceased individuals. There are two classes of dental radiographs. radiographs acquired after the death, post-mortem (PM) radiographs, and radiographs acquired while the person is alive, ante-mortem (AM) radiographs, see Fig. 3.1.

AM radiographs, labeled with patient names, are collected from the dentist. The method used in dental biometrics is matching unlabeled PM radiographs against a database of labeled AM radiographs. The identity of the PM radiograph is obtained, if the dental features in a PM radiograph sufficiently match with the dental features from the AM radiograph [18, 3].

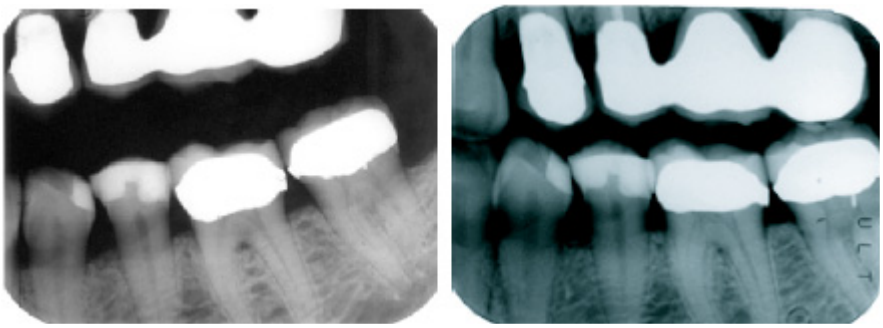

(a) (b)

Figure 3.1: (a) Ante-mortem (AM) and (b) post-mortem (PM) radiograph of an individual [3].

3.2 Forensic Odontology (Forensic Dentistry)

Forensic odontology (forensic dentistry) is the branch of forensics concerned with identifying human individuals based on their dental features and has a history of more than two centuries [18]. This involves interaction with law enforcement agencies charged with the responsibility of investigating the evidence from cases involving violent crime, child abuse, elder abuse, missing persons and mass disaster scenarios [19]. Even if only a little dental information is available, an opinion can still be offered on age, habits, oral hygiene, and individual features which may match with ante-mortem records [20].

3.2.1 Categories of Dental Evidence

Different types of dental evidence in the field of forensic odontology are [19]:

- A human tooth or tooth fragment.
- A fragment of a human jawbone.
- DNA obtained from a tooth, toothbrush, cigarette, etc.
- DNA obtained from a swabbing of bite marks, foodstuff or object that possesses saliva transfer evidence.
- Dental restorations and appliances that can be associated to a particular person through name inscriptions, specific dental material type, composition or unusual design characteristics.

3.2.2 Legal Issues in Forensic Odontology

Radiology results are important information in a dental practice and are considered as definitive evidence in court or identification cases. Since radiology is widely used to record and evaluate the findings, it is also recommended by United Nations, Interpol and American Board of Forensic Odontology in investigations of mass graves, disasters and victim and body identification [21].

The combinations of restored, non-restored, missing, and decayed teeth can be as unique as a fingerprint and the probability of two dentitions being the same is very low. This uniqueness allows for dental comparison to be a legally acceptable means of identification, even if only one tooth remains [22].

3.2.3 Usage of Dental Biometrics

Currently, identification relies on a manual comparison between the AM and PM dental radiographs and is based on a systematic dental chart prepared by forensic experts. Distinctive features for each individual tooth are noted in this chart. These features include properties of teeth (e.g. tooth present or not present, crown and root morphology, pathology and dental restorations), periodontal tissue features and anatomical features. The forensic expert rejects or confirms the tentative identity depending on the number of matches in the dental chart [4, 18].

There are two main advantages to automate this procedure. First, an automatic process will be able to compare the PM records against AM records objectively and quantitatively to determine the closest match of multiple identities and second, an automatic (or semi-automatic) system can perform identification on a large database while a manual (or non-automated) system is useful for verification on small data sets only [4].

3.3 Teeth as Biometric Characteristics

Behavioral characteristics (e.g. speech or signature) as well as most physical characteristics are not appropriate for PM identification. Especially under severe circumstances encountered in mass disasters (e.g. airplane crashes, fires accidents, etc.) or when there is no identification possible within a couple of weeks postmortem. Therefore, a postmortem biometric characteristic has to survive severe conditions and resist early decay that affects body tissues. Dental features are considered the best candidates for PM identification because of their survivability [18, 3]. Tooth shapes, appearances, tooth fragments, metal restorations, skull and jawbone fragments may possess features that can be associated with just one person [19].

3.3.1 Universal Numbering System

The Universal Numbering System is a method of identifying teeth and is approved by the American Dental Association. This method employs numbers with each tooth designated by a separate number from 1 to 32 [23]. Figure 3.2 illustrates the numbering system used on a standard dental chart for a full set of adult teeth.

The human permanent dentition is divided into four classes of teeth based on appearance and function or position [23]:

1. **Incisors**, are located in the front of the mouth and have sharp, thin edges for cutting. The lingual surface can have a shovel-shaped appearance.
2. **Cuspids** (canines or eyeteeth) are at the angles of the mouth. Each has a single cusp in stead of an incisal edge and are designed for cutting and tearing.
3. **Bicuspids** (premolars) are similar to the cuspids but they have two cusps used for cutting and tearing, and an occlusal surface to crush food.
4. **Molars** are located in the back of the mouth. Their size gradually gets smaller from the first to third molar. Each molar has four or five cusps, is shorter and blunter in shape than other teeth and provides a broad surface for grinding and chewing solid masses of food.

The teeth of the upper arch are called maxillary teeth (upper teeth) because their roots are embedded within the alveolar process of the maxilla (upper jaw). Those of the lower arch are called mandibular teeth (lower teeth) because their roots are embedded within the alveolar process of the mandible (lower jaw). Each arch contains 16 teeth and is divided into a right and left quadrant. Teeth are described as being located in one of the four quadrants. A human receives normally two sets of teeth during a lifetime. The primary set, which usually consists of 20 teeth and a permanent set which usually consists of 32 teeth. In each quadrant, there are eight permanent teeth: two incisors, one cuspid, two bicuspids, and three molars [23], see Fig. 3.3.

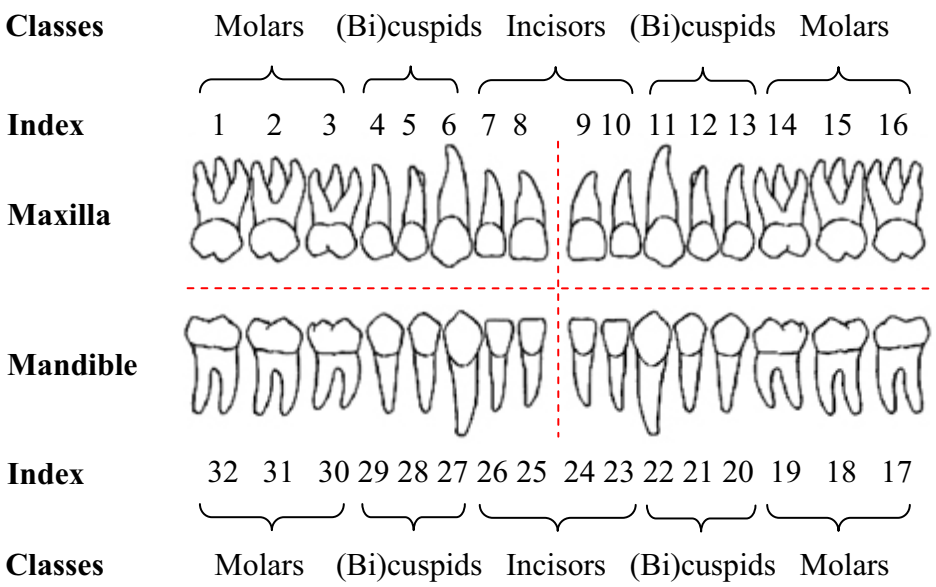

Figure 3.2: Universal Numbering System used on a standard dental chart for a full set of adult teeth.

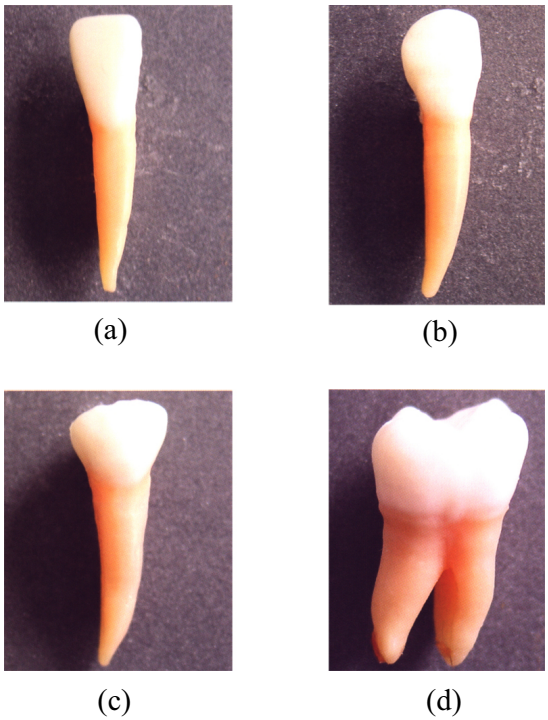

Figure 3.3: Photographs of different types of teeth. (a) Adult mandibular right central incisor, (b) Adult mandibular right cuspid, (c) Adult mandibular right first bicuspid, (d) Adult mandibular right second molar [19].

3.3.2 Dental Restorations (Dental Works)

Dental restoration refers to the reproduction of missing tooth structure through the use of artificial materials. There are a number of benefits for tooth restoration which include health advantages (the strengthening of affected teeth to prevent further tooth erosion, the replacement of damaged and/or missing teeth) and aesthetical advantages (replacement of a damaged tooth with a more natural, healthier looking tooth) [24].

There are two ways to perform dental restorations:

- **Direct restorations** are fillings which are placed immediately into a prepared cavity into the tooth. Common direct restoration materials include dental amalgam, composite resins and glass ionomer cement (tooth-colored materials that bond chemically to dental hard tissues).
- **Indirect restorations** are custom made fillings that are created in a dental laboratory according to a doctor's prescription. Common indirect restorative materials include acrylic, porcelain, zircon, gold and other metals.

Different Types of Dental Restorations are [24, 25]:

- **Amalgam fillings:** Amalgam is produced by mixing mercury and other metals and is still the most commonly used filling material because it is durable, easy to use and inexpensive.
- **Composite resin fillings:** A tooth-colored filling material used primarily for front teeth. Although cosmetically superior, it is generally less durable than other materials.
- **Cast restorations:** A procedure that uses a model of the tooth (an impression) to make a casting which replaces missing parts (e.g. crowns).
- **Crowns (or caps):** The artificial covering of a tooth with metal, porcelain of porcelain fused to metal. Crowns cover teeth weakened by decay or severely damaged or chipped.
- **Inlays and onlays:** An inlay is a solid filling cast to fit the missing portion of the tooth and cemented into place. An onlay is a partial crown and covers one or more tooth cusps.
- **Implants:** A dental implant is an artificial tooth root surgically placed directly into the jawbone where a tooth is missing. They are used to support dental prosthesis from single crowns to full denture.

3.3.3 Types of Dental Radiographs

There are three major types of dental radiographs called panoramic, bitewing and periapical images.

Panoramic Dental Radiographs

A panoramic dental radiograph is a large, single x-ray film that shows the bony structure of the teeth and face, see Fig. 3.4. This type of radiograph differs from the others because it is entirely extraoral, which means that the film remains outside of the mouth while the machine shoots the beam. A much wider area than any intra oral film can be seen on the radiograph including bony tumors, cysts and the position of the wisdom teeth as well as structures outside the mouth like the sinuses (air-filled cavities in a skull bone) and the temporomandibular joints that hinge the mandible to the skull.

The panoramic dental radiograph is a lower resolution image than intraoral films. This means that the individual structures which appear on them, such as the teeth and bones, are somewhat fuzzy and structures like caries (tooth decay) are imaged without the fine detail seen on intraoral films. They are not considered sufficient for the diagnosis of decay, and must be accompanied by a set of bitewing radiographs if they are to be used as an aid for full diagnostic purposes. In addition to medical and dental uses, panoramic films are especially good for forensic purposes [26].

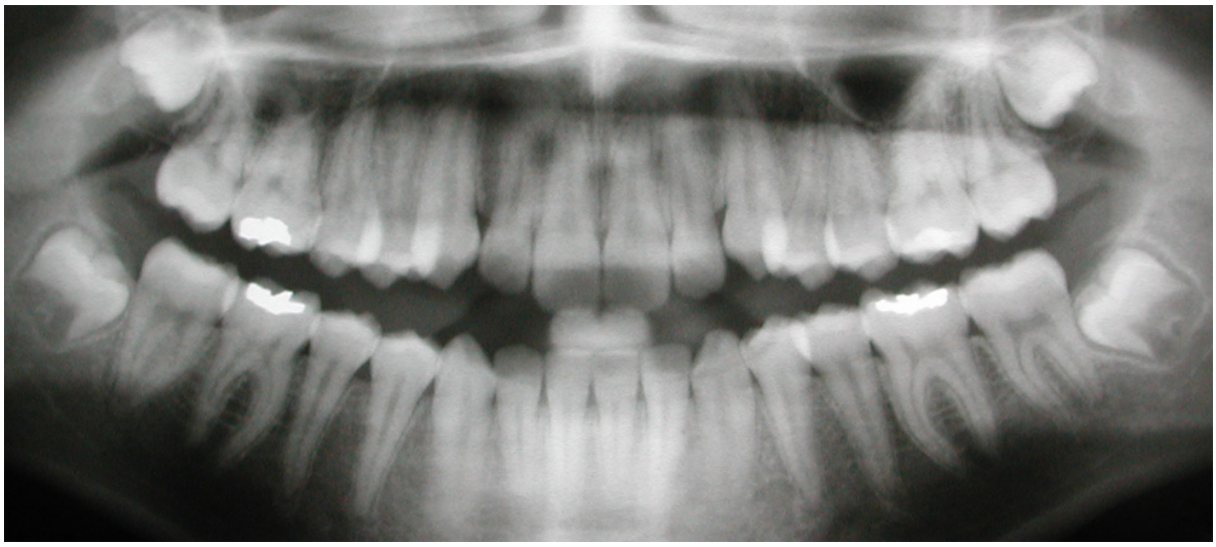

Figure 3.4: Panoramic dental radiograph including dental restorations.

Bitewing Dental Radiographs

A bitewing dental radiograph is taken mainly of the back teeth (molars and bicuspids) while the patient bites the teeth together; thus, the film contains images of both, the upper and lower teeth, see Fig. 3.5(a). All three elements (the teeth, the film, and the x-ray beam) are optimized to give the most undistorted shadows possible. The film and teeth are parallel, and the beam is aimed directly at both at a 90 degree angle. Thus, bitewing films afford the most accurate representation of the true shape of the teeth and associated structures such as decay, fillings, shape of nerves and bone levels [26].

Periapical Dental Radiographs

A periapical dental radiograph is shot from an angle in which the three elements (the teeth, the film, and the x-ray beam) are not necessarily aligned parallelly. They can show the whole tooth, including the crown which is above and the root which is below the gumline, see Fig. 3.5(b). Some distortion is introduced on purpose to be sure that the shadow of the entire tooth or teeth falls on the film. This is done because in many instances, the space available in the mouth or the curvature of the roof of the mouth will not permit parallel placement of the film [26].

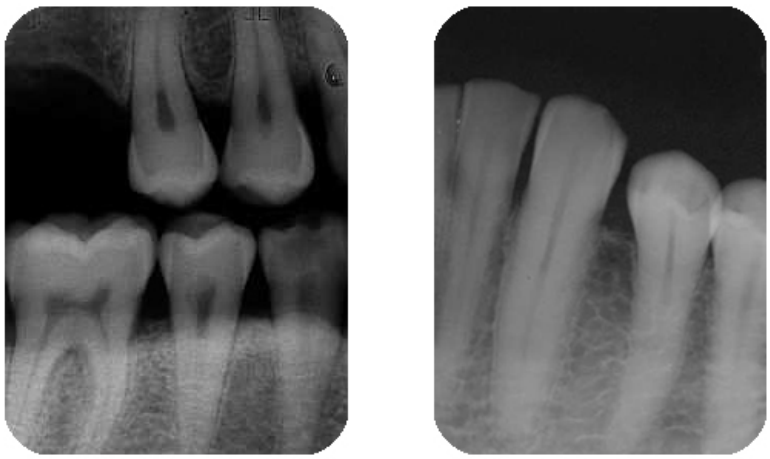

(a) (b)

Figure 3.5: Kinds of dental radiographs. (a) Bitewing and (b) periapical dental radiograph [27].

3.3.4 Resistance of Teeth and Dental Restorations

The radiographic evaluation of dental remains, especially after an exposure to fire, is a significant aspect in the field of forensic dentistry. *C. Savio et al.* presented a study [21] in which an evaluation of radiographic features of unrestored, endodontically treated and restored teeth after exposure to an experimental range of high temperatures was performed.

Teeth are components that often survive severe fires because of their particularly resistant composition, influenced by the protection given by the soft tissues of the face and other materials or elements sometimes present (e.g. glasses, crash helmet). Teeth show damages caused by heat related to the oxidant's nature, the combustion's duration and the action of different fire extinguishing products used. In some cases, only fragments of teeth are available for the identification. For this, it is therefore more important to obtain their radiographs for a comparison as suggested by the American Board of Forensic Odontology (ABFO) guidelines [21, 28].

Results for Unrestored Teeth

From the results of the study, it is possible to say that restored and unrestored teeth were not strongly affected by temperature exposure below 200 °C (392 °F). Above 200 °C (392 °F), the teeth were affected by a progressive formation of fissures and many crowns crushing were recorded. The radiographic properties of the roots were available for analysis up to 1100 °C (2012 °F). An example of an unrestored tooth before and after thermal stress can be seen in Fig. 3.6.

Figure 3.6: An unrestored tooth (a) before and (b) after thermal stress (800 °C-1472 °F) [21].

Results for Restored Teeth

The same behavior of the dental tissues for unrestored teeth can be seen in the restored teeth. Although many crowns crushed, a number of significant radiographic details were conserved because the composite fillings were in place maintaining the shape up to 600 °C (1112 °F) (see Fig. 3.7), the amalgam fillings were in place maintaining the shape up to 1000 °C (1832 °F) (see Fig. 3.8) and the endodontic (or root canal) treatments were recognizable up to 1100 °C (2012 °F).

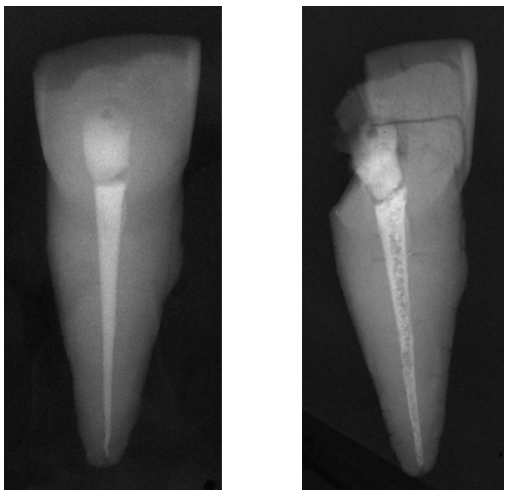

Figure 3.7: An endodontically treated tooth restored with a composite filling (a) before and (b) after thermal stress (600 °C-1112 °F) [21].

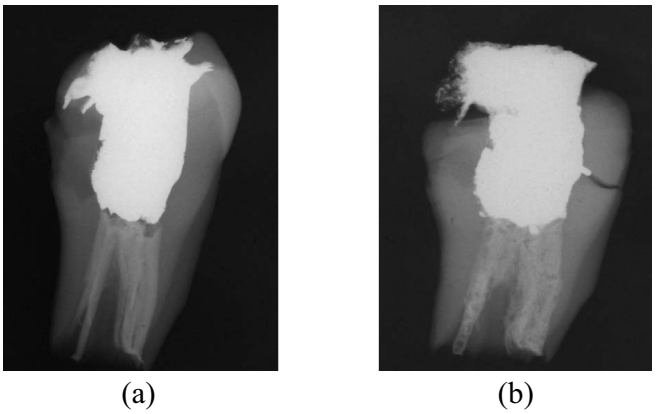

Figure 3.8: An endodontically treated tooth restored with amalgam filling (a) before and (b) after thermal stress (1000 °C-1832 °F) [21].

According to the evaluation of *C. Savio et al.*, it can be said that teeth and also dental restorations can be used as good biometric characteristics after an exposure to fire and high temperatures.

3.4 Related Works

According to experts from the Criminal Justice Information Services Division (CJIS) of the FBI, there are 100,000 unsolved cases of missing persons at any given point in time. In 1997, The CJIS of the FBI created a dental task force (DTF) whose goal is to improve the utilization and effectiveness of the National Crime Information Center's (NCIC) missing and unidentified persons (MUP) files. The DTF recommended the creation of a Digital Image Repository (DIR) and an Automated Dental Identification System (ADIS) with goals and objectives similar to the Automated Fingerprint Identification System (AFIS) but using dental characteristics instead of fingerprints [1].

According to these facts, much work has been done in the field of dental biometrics:

- *Mahoor* and *Abdel-Mottaleb* [29] proposed a method to obtain the indices of teeth in bitewing dental radiographs by using Bayesian classification. The algorithm considers the arrangement of the teeth in the jaw and assigns a number based on the Universal Numbering System. A major limitation of their method is that bitewing images contain only molars and bicuspids teeth. They also assume that there are no missing teeth in the radiographs, which is not generally true in general. If this assumption is not satisfied, registration errors will occur.

- *Nazmy, Nabil, Salam* and *Samy* [30] proposed a set of enhancing techniques to improve the poor quality of dental radiographs using morphological algorithms such as top and bottom hat transforms and flood fill algorithms. These techniques provide images that can be segmented using morphological methods. Each tooth is extracted from a set of teeth using the watershed technique. The matching process depends on geometric features and on a signature which is invariant to translation, scaling and rotation, and is produced by a pulse coupled neural network (PCNN).

- *Said, Fahmy, Nassar* and *Ammar* [1] proposed a method for the segmentation of dental radiographs by using an algorithm based on a morphological filtering and a modified 2-D wavelet transform. Their work addresses the problem of identifying each individual tooth and how the contours of each tooth can be extracted. Therefore, they perform integral projection of horizontal and vertical lines to detect the boundaries of the teeth.

- *Anil K. Jain* and *Hong Chen* proposed an algorithm for the registration of the dental atlas to dental radiographs [27] and also a method of matching dental x-ray images for human identification [3, 4, 27, 31]. More detailed descriptions of these algorithms are presented in the following two sections.

3.4.1 Registration of the Dental Atlas to Radiographs for Human Identification (*Anil K. Jain, Hong Chen*)

Registering a dental radiograph to the dental atlas (Universal Numbering System) reveals the position and index of each tooth in the radiograph. This is used to establish the correspondence of teeth when matching two dental radiographs. The proposed method deals with all three types of radiographs (bitewing, periapical and panoramic images). The first stage of the algorithm is to classify the teeth in the radiographs into molars, (bi)cuspids and incisors. Therefore, three Support Vector Machines (SVM) are fused to obtain good classification accuracy. The second stage uses a Hidden Markov Model (HMM) to represent the dental atlas. The observed sequences in the radiographs are registered to the dental atlas by searching for the path that has the largest probability of occurrence. Results of this method can be seen in Fig. 3.9.

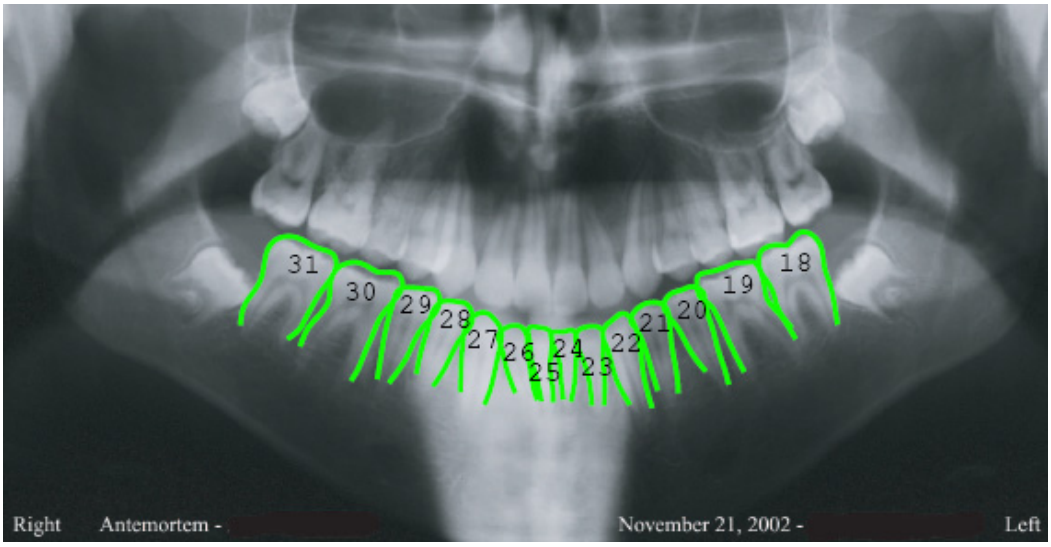

Figure 3.9: Result of a registration of the dental atlas (of the lower teeth) to a panoramic dental radiograph [27].

3.4.2 Matching of Dental X-ray Images for Human Identification (*Anil K. Jain, Hong Chen*)

The goal of this work addresses the problem of automating the process of identifying people based on their dental radiographs. The system consists of two main stages: the feature extraction stage, where the tooth contours are extracted, and the feature matching stage, where the extracted tooth contours are compared against tooth contours stored in a database. The first step is to segment the radiograph into blocks such that each block has a tooth in it, see Fig. 3.10(a). To extract the tooth contours (see Fig. 3.10(b)),

a probabilistic model is used to describe the distribution of tooth and background pixels. After that, transformations align the contours to correct imaging geometric variations.

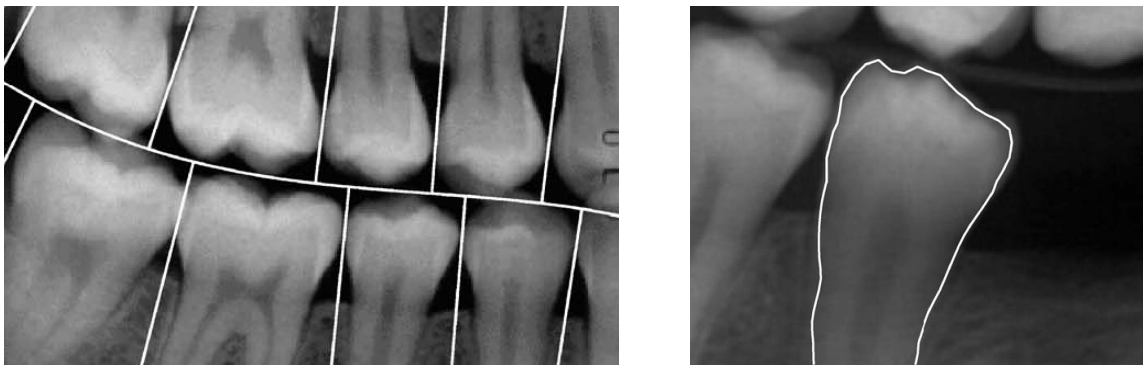

Figure 3.10: Feature extraction of dental radiographs. (a) Result of separating the teeth into blocks. (b) Extracted tooth contour [4].

The dental works, which appear as bright regions in the radiographs, are salient features for subject identification. To extract the contours of the dental work, they used the intensity histogram of the tooth image and approximated it with a mixture of Gaussians model, where the Gaussian component with the largest mean value corresponds to the pixels associated with the dental work. Anisotropic diffusion is used which smoothes the pixels inside each region while preserving the boundary between the regions, see Fig 3.11.

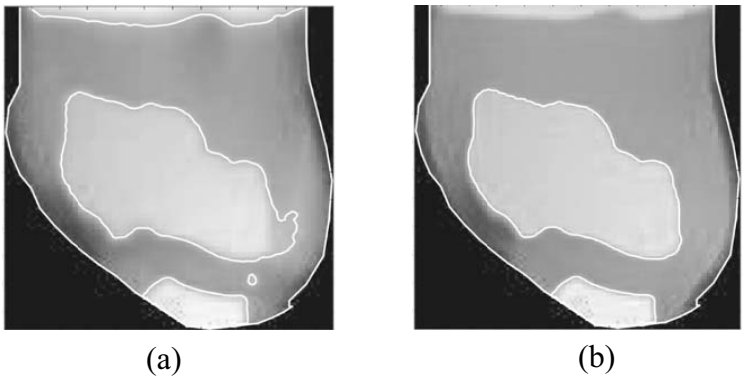

Figure 3.11: Tooth including the extracted contours of the dental works (a) before and (b) after using anisotropic diffusion to smooth the pixels inside each region [3].

Finally, matching scores for the tooth and the dental works contours are computed. The combination of these matching scores measures the similarity between the two given radiographs. A candidate list of potential matches is generated for human experts to make further decisions.

3.4.3 Problems using Dental Biometrics

Dealing with dental biometrics leads to several problems:

- Unlike other biometric characteristics (e.g. fingerprint or iris) dental features do change over time, e.g. teeth and dental restorations can change their appearance or can be missing altogether after the AM radiographs are acquired. For this reason, dental based identification is considered less reliable than other biometric methods but may be the only available biometric method in certain cases (e.g. fires accidents) [32].
- The feature extraction is a difficult problem for matching dental radiographs, especially if they have a poor quality and some tooth or dental restorations contours cannot be correctly detected.
- Dental radiographs may be acquired with different viewing angles. This may affect the matching process of a post-mortem (PM) with an ante-mortem (AM) radiograph [27].
- It is extremely difficult to build a dental chart automatically, which is currently done by forensic experts manually, because each tooth has to be detected and classified before it can be processed.
- Different dental radiographs have different resolutions, orientations and luminance properties, depending on the X-ray machine and the dentist who took it [1].

Chapter 4

Image Processing and Algorithms

The following chapter provides an overview of Snakes and the Levenshtein distance that are used in the proposed dental biometric method. A "snake" is an active contour algorithm which can be used when dealing with missing boundary information or noisy images to find unclear borders. The Levenshtein distance is the smallest number of operations (insertions, deletions and substitutions) required to change one string or tree into another and therefore presents a measure for the similarity of dental radiographs.

4.1 Snakes

A snake is an energy minimizing curve guided by external constraint forces and influenced by image forces that pull it toward features such as lines and edges [33]. The curve can be represented as a spline that is a polynomial or set of polynomials used to describe or approximate curves and surfaces.

4.1.1 Introduction

The algorithm used in this work was introduced from *Kass et al.* in 1987 and has great importance in applications like segmentation, edge detection and tracking. Snakes can fill in missing boundary information and are very robust against noise which make them very useful in a wide range of computer vision applications. In the following the algorithm from *Kass* [33], *Xu* and *Prince* [34, 35, 36] is presented.

4.1.2 Mathematical Definition of Snakes

Snakes are curves defined within an image domain that can move under the influence of internal forces (elasticity and bending forces) coming from within the curve itself, and external forces (potential and pressure forces) computed from the image data [35]. A

snake is a parameterized curve $\mathbf{x}(s) = (x(s)\ y(s))^T$, where *x(s)*, *y(s)* are x, y coordinates along the contour and s ranges from 0 to 1. A snake is minimizing the energy functional

$$E = \int_0^1 E_{int}(\mathbf{x}(s)) + E_{ext}(\mathbf{x}(s))ds \tag{4.1}$$

$$E_{int} = \frac{1}{2}[\alpha \mid \mathbf{x}'(s) \mid^2 + \beta \mid \mathbf{x}''(s) \mid^2] \tag{4.2}$$

by moving through the spatial domain of an image. E_{int} represents the internal energy per unit length of the spline due to bending. The weighting parameters α and β are used to define the smoothness and the elasticity properties of the curve. Setting $\beta(s)$ to zero at a appoint allows the snake to become second-order discontinuous and develop a corner. $\mathbf{x}'(s)$ and $\mathbf{x}''(s)$ denote the first and second derivative of $\mathbf{x}(s)$ with respect to s. The first-order term makes the snake act like a membrane and the second-order term makes it act like a thin plane. The external energy E_{ext} should have small values on features that represent object boundaries.

$$E_{ext}(x, y) = - \mid \nabla(G_\sigma(x, y) * I(x, y)) \mid \tag{4.3}$$

(4.3) is an example for an external energy function E_{ext} for a gray level image $I(x, y)$. The term $G_\sigma(x, y)$ is a two-dimensional Gaussian function with standard deviation σ and ∇ is the gradient operator. Large values of σ will cause the boundaries to become blurry. However, such large σ's are often necessary in order to increase the capture range around the object boundary of the snake. The Euler equation (differential equations of the type $x^2y'' + \alpha xy' + \beta y = 0$)

$$\underbrace{\alpha\mathbf{x}''(s) - \beta\mathbf{x}''''(s)}_{F_{int}} \underbrace{-\nabla E_{ext}}_{F_{ext}} = 0 \tag{4.4}$$

must be satisfied when a snake minimizes E. Each iteration effectively takes implicit Euler steps with respect to the internal energy and explicit Euler steps with respect to the image and external energy. The numeric considerations are relatively important. In a fully explicit Euler method, it takes $O(n^2)$ iterations each of $O(n)$ time for an impulse to travel down the length of a snake. The resulting snakes are flaccid. In order to erect more rigid snakes, a more vital and stable semi-implicit method that accommodates the large internal forces is used. This method allows forces to travel the entire length of a snake in a single $O(n)$ iteration. (4.4) is equivalent to the force balance equation

$$F_{int} + F_{ext} = 0. \tag{4.5}$$

The internal force $F_{int} = \alpha \mathbf{x}''(s) - \beta \mathbf{x}''''(s)$ controls the ability of stretching and bending of the snake whereas the external force $F_{ext} = -\nabla E_{ext}$ pulls the snake towards the image edges. To make the snake dynamic and to solve (4.4), $\mathbf{x}(s)$ is treated as a function of length s and time t respectively, $\mathbf{x}(s,t)$. Then, the partial derivative of $\mathbf{x}(s,t)$ with respect to t is set equal to the left hand side of (4.4) which results in

$$\mathbf{x}_t(s,t) = \alpha \mathbf{x}''(s,t) - \beta \mathbf{x}''''(s,t) - \nabla E_{ext}. \tag{4.6}$$

When the solution $\mathbf{x}(s,t)$ stabilizes, the term $\mathbf{x}_t(s,t)$ vanishes and a solution of (4.4) is achieved. A numerical solution of (4.6) can be found by discretizing the equation and solving the discrete system iteratively.

4.1.3 Gradient Vector Flow (GVF) Fields and GVF Snakes

Traditional snakes[1] suffer from two main key difficulties: At first they have difficulties to converge to concave boundary because the magnitudes of the external force die out very rapidly away from the object boundary as can be seen in Fig. 4.1. The second problem is that the initial contour of the snake has to be close to the true boundary.

A new approach for snakes was presented by *Xu* and *Prince* [35] in the year 1998. They proposed an alternative way to compute an external force field. They call these fields gradient vector flow (GVF) fields. Snakes that use GVF fields as the external force field are called GVF snakes. The GVF field has large external forces far away from the object boundaries which increases the capture range of the snake. The standard external force F_{ext} in (4.5) is replaced with the new static external force $F_{ext}^{(g)} = \mathbf{v}(x,y)$ which does not change with time or depend on the position of the snake itself. The external potential force $-\nabla E_{ext}$ in (4.6) is replaced with $\mathbf{v}$ which gives the equation

$$\mathbf{x}_t(s,t) = \alpha \mathbf{x}''(s,t) - \beta \mathbf{x}''''(s,t) + \mathbf{v}. \tag{4.7}$$

[1] In this case parametric active contour algorithm; literature distinguishes between parametric and geometric active contours. Parametric active contours are represented explicitly as parameterized contours within an image domain and allow them to move toward desired features. Geometric active contours are represented implicitly as the zero-level sets of higher-dimensional surfaces. The updating is performed on the surface function within the entire image domain [36].

The process starts by calculating an edge map of the given image. According to the gradients of the edge map, the GVF field is produced.

Edge Map

At first an edge map $f(x, y)$ derived from the given image $I(x, y)$ is defined as having the property that it is larger near the image edges or at the desired features. Any binary or gray-level edge map defined in the image processing literature [37] can be used.

The defined edge map has three features that are important for the snake formation:

1. The gradient of the edge map f has vectors pointing towards the edges. These vectors are normal to the edges at the edges. This means an initialized snake close to the edge will stabilize near the edge, which is preferred.
2. These vectors generally have large magnitudes only in the immediate vicinity of the edges. Because of this property, the capture range of the snake will be very small in general.
3. In homogenous regions where $I(x, y)$ is nearly constant, f is almost zero. This means that within homogenous regions the external forces are small.

The first property of the gradients near the edges is highly desirable, whereas the last two properties are contra productive for the snake. To reduce the effects of the last two properties, a diffusion process is used to extend the gradient map farther away into the homogenous regions. As an important benefit, vectors that point into boundary concavities are also created out of the diffusion process.

GVF Field

The GVF field is defined as the vector field $\mathbf{v}(x, y) = (u(x, y)\ v(x, y))^T = (u\ v)^T$ that minimizes the energy functional

$$\varepsilon = \iint \mu(u_x^2 + u_y^2 + v_x^2 + v_y^2) + \mid \nabla f \mid^2 \mid \mathbf{v} - \nabla f \mid^2 dx\, dy. \tag{4.8}$$

The first term in (4.8) smoothes the vector field $\mathbf{v}$, whereas the parameter μ is a constant regularization parameter which adjusts the tradeoff between the first and the second term in the integrant in (4.8). This parameter should be set according to the noise level in the image, i.e., a high μ is needed for noisy images. When the gradient $\mid \nabla f \mid$ in the second term in (4.8) is small, the first term, including the sum of the squares of the partial derivatives of the vector field $\mathbf{v}$, dominates the energy. This causes a low variation of the vector field $\mathbf{v}$. A large $\mid \nabla f \mid$ has the effect that the second term dominates the integrand.

The second term is minimized by setting $\mathbf{v} = \nabla f$, which produces two desired effects:

1. $\mathbf{v}$ is kept nearly equal to the gradient of the edge map and
2. $\mathbf{v}$ is kept slowly varying at the homogenous regions of the image.

The GVF field can be found by solving the pair of Euler equations

$$\mu\nabla^2 u - (u - f_x)(f_x^2 + f_y^2) = 0 \tag{4.9}$$
$$\mu\nabla^2 v - (v - f_y)(f_x^2 + f_y^2) = 0 \tag{4.10}$$

by using calculus variations [35] where ∇^2 is the Laplacian operator. Calculus of variations seeks to find the path, curve or surface, for which a given function has a stationary value (which, in physical problems, is usually a minimum or maximum). Mathematically, this involves finding stationary values of integrals [38]. It is noted that in a homogeneous region, where $I(x, y)$ is constant, the second term in each equation is zero because the gradient of $f(x, y)$ is zero. Therefore, within such a region, u and v are each determined by Laplace's equation, and the resulting GVF field is interpolated from the region's boundary, reflecting a kind of competition among the boundary vectors. This explains why GVF yields vectors that point into boundary concavities.

4.1.4 Comparison between Traditional Snakes and GVF Snakes

GVF snakes address the problems of traditional snakes by using a new class of external forces An advantage of GVF snakes over traditional snakes algorithms is the ability to move into boundary concavities, see Fig. 4.2(a). They also have a larger capture range as can be seen in Fig. 4.2(b) and 4.2(c), which makes them more insensitive to initialization. The initialization of the snake can be inside, outside or across the object's boundary, see Fig. 4.3. A drawback of GVF Snakes in comparison to traditional snakes is its large computational cost which makes the algorithm unqualified for real time applications like tracking.

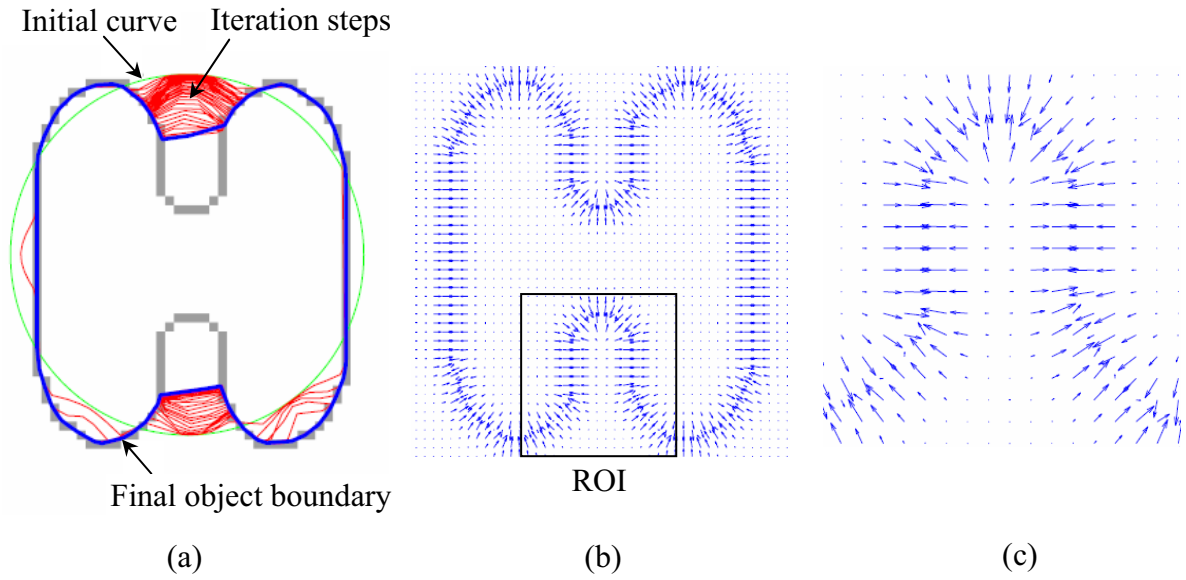

Figure 4.1: Traditional snake witch (a) that does not converge to the concave boundary (after 150 iteration steps); (b) The external force field dies out rapidly away from the object boundary; (c) Close-up of the region of interest (ROI) marked in the external force field in (b).

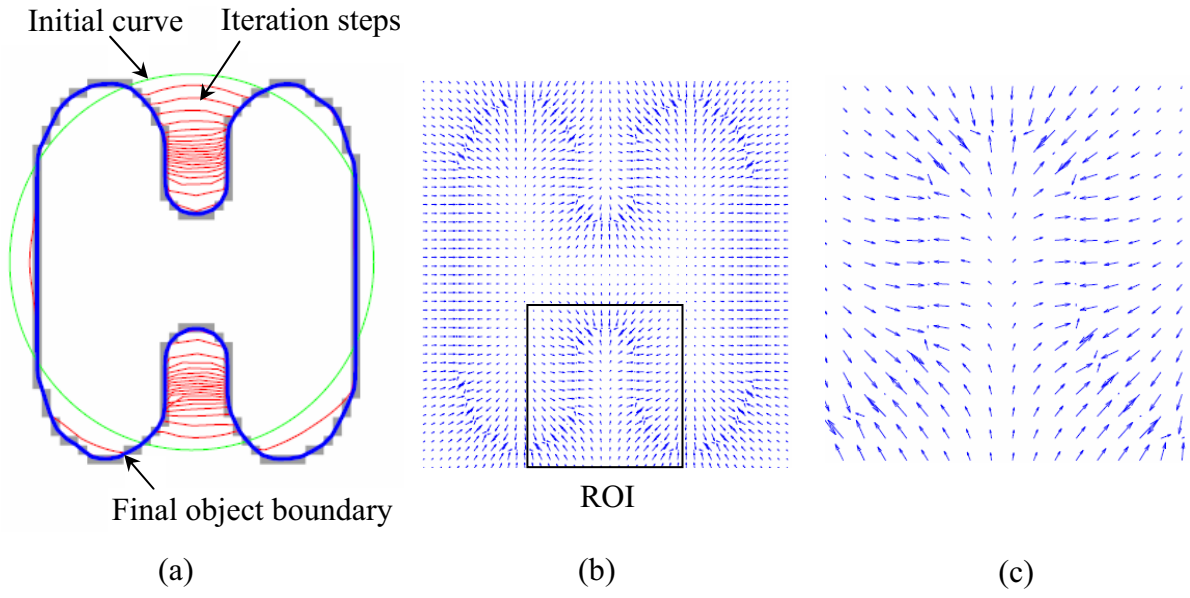

Figure 4.2: A GVF snake which converge to boundary concavities (after 150 iteration steps); (b) GVF field with larger capture range than traditional snakes; (c) Close-up the region of interest (ROI) marked in the GVF field in (b).

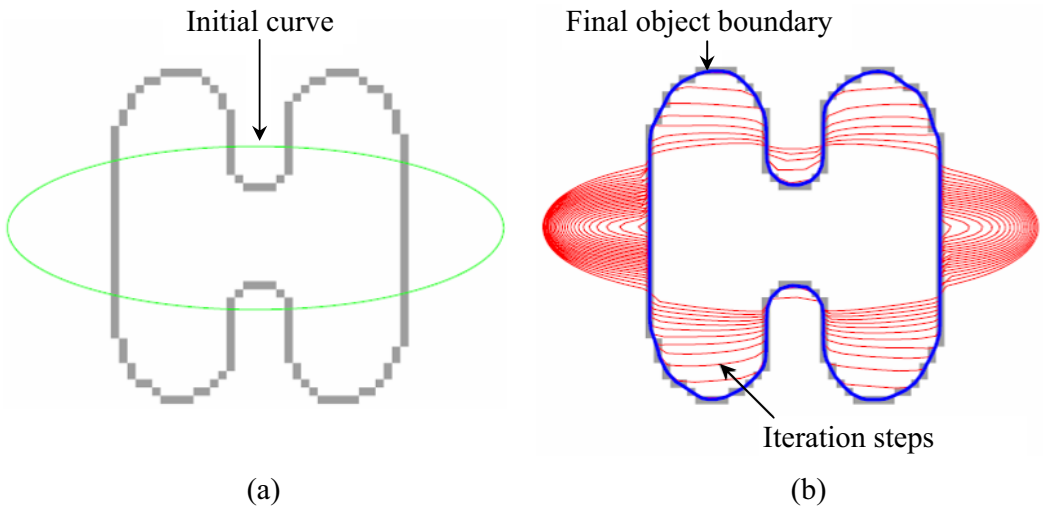

Figure 4.3: Initialization of a GVF Snake (a) across the object's boundary; (b) Correctly found object boundary after 150 iteration steps.

4.1.5 Advantages and Drawbacks of Snakes

Snakes have several advantages over classical feature extraction techniques but are not without their drawbacks [39]:

Advantages:

- The first term in (4.8) works as a noise filter which makes snakes insensitive up to a certain level of noise and other ambiguities in the image.
- The initial curves can be placed automatically or interactively by the user.
- The feature extraction procedure works autonomously during the search for a minimal energy state.
- Dynamic objects in temporal and spatial dimensions can be tracked.
- Not connected structures can be detected.

Drawbacks:

- Snakes need an initialization curve to start the iteration process which should not be too far away from the desired features.
- The accuracy of the solution is dependent on the convergence criteria used in the energy minimization technique.
- The tighter the convergence criteria, the higher the computational costs.
- The speed of execution makes them unqualified for real time applications.

4.2 Levenshtein Distance (Edit Distance)

In many applications it is necessary to find out the similarity between two strings. A widely-used algorithm to solve this problem is called Levenshtein distance or Edit distance. The algorithm was developed by *Vladimir Levenshtein* in 1965 and is defined by the smallest number of insertions, deletions and substitutions required to transform one string or tree into another [40]. The higher the Levenshtein distance, the higher is the difference between the two strings.

The Levenshtein distance can be implemented by using dynamic programming. Dynamic programming was first presented by *Richard Bellman* in the year 1940 and describes a way of solving problems where the best decision is found one after another. In comparison to the Hamming distance, which is only defined for strings of the same length, the Levenshtein distance is more sophisticated because strings of arbitrary lengths can be used.

4.2.1 The Algorithm

To implement the algorithm using linear programming approach, a 2-dimensional function $\mathbf{D}(i, j)$ of the size N x M is used, where N and M denote the lengths of the two input strings s and t respectively. $\mathbf{D}(0 \ldots N, 0)$ is initialized with natural numbers from 0 to N. $\mathbf{D}(0, 0..M)$ is initialized from 0 to M as can be seen in the flowchart of Fig. 4.4.

A double-loop is used to examine each character of s (i from 1 to N) and each character of t (j from 1 to M). If the i'th character of the string s, called $s(i)$, is equal to the character j of the string t, called $t(j)$, the cost is set to zero. If the compared characters are not equal, the cost is set to one, see Fig. 4.4.

In the next step, the element $\mathbf{D}(i, j)$ is assigned to the minimum value out of:

1. The cell above plus one (deletion)
2. The cell to the left plus one (insertion)
3. The cell diagonally above and to the left plus the cost (substitution)

After all iteration steps are completed, the final Levenshtein distance (LD) is found in $\mathbf{D}(N, M)$ as can be seen in Fig. 4.4.

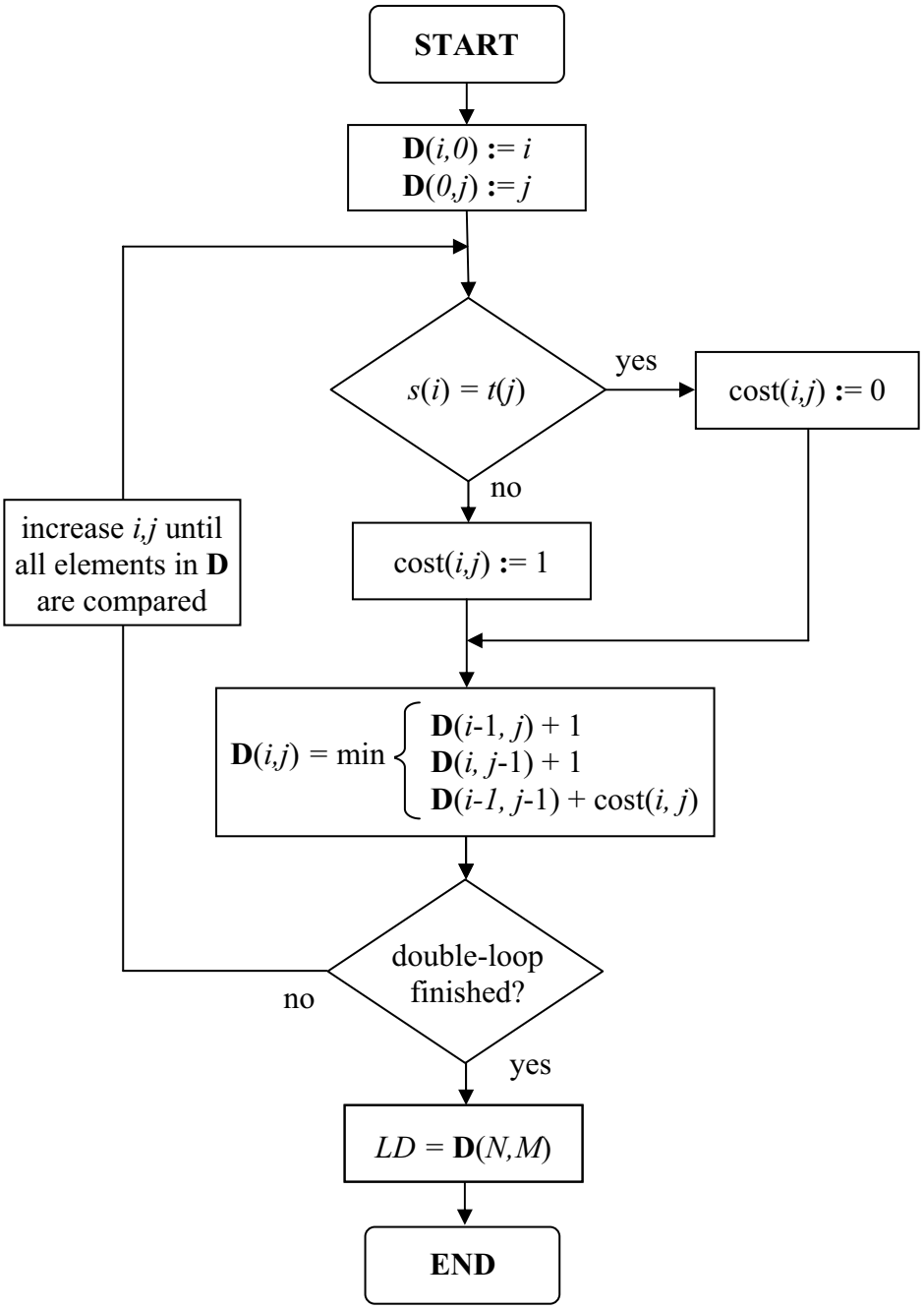

Figure 4.4: Flowchart of the algorithm that calculates the Levenshtein distance (LD).

Complexity

The time-complexity of the algorithm is $O(\mid s \mid \cdot \mid t \mid)$ which means $O(n^2)$, if the strings s and t have a length of about n. If the matrix $\mathbf{D}$ is kept for tracing the transformation steps of the strings as it is illustrated in the example of Fig. 4.5, the space-complexity is also $O(n^2)$. This can be used to find an optimal alignment of the elements [41].

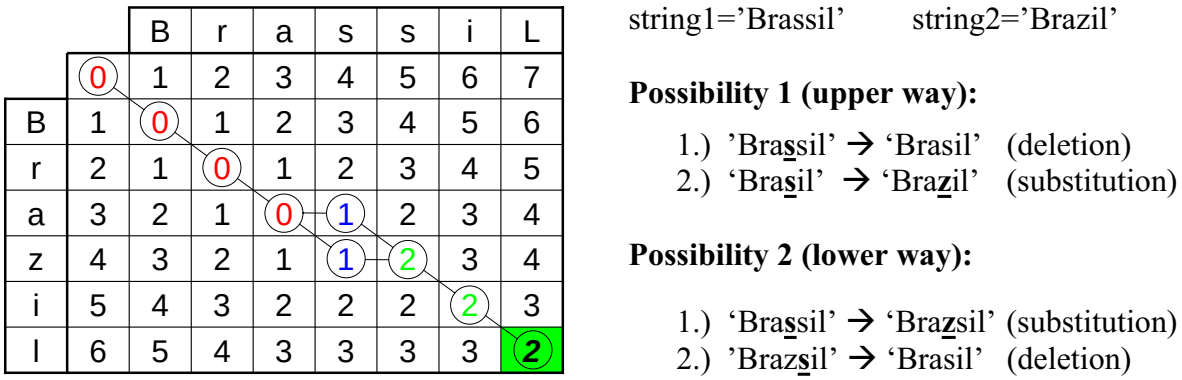

Figure 4.5: Computation of the Levenshtein distance including all transformation steps for tracing. There are two different possibilities to transform the string1 which is 'Brassil' into string2 which is 'Brazil'. The total number of operations is given by two, in both cases.

4.2.2 Variations

Possible variations for adjusting the algorithm for special applications include:

- The penalty costs of the operations insertion, deletion and substitution can be varied.
- The number of different operations can be stored separately.
- If only the value of the Levenshtein distance is needed, the space-complexity can be improved to $O(\mid s \mid)$ by using only the two bottom most rows of the matrix for each step.

4.2.3 Applications

The Levenshtein distance is used in applications including [41]:

- **Spelling correction / Spell checking:** If a written text contains words, which are not in the used dictionary but are close to other known words, possible corrections can be suggested.
- **Speech recognition:** To find a close match between a new word/syllable and one in a library stored word/syllable.
- **DNA analysis:** Computation of a distance between DNA or protein sequences to find genes or proteins that may have shared functions or properties.
- **Plagiarism detection:** Indication of similarity in literature or scientific works.

Chapter 5

Methods

The following chapter explains the proposed dental biometric identification method in detail. The three main processing stages include feature extraction, creation of a dental code and feature matching. The process of creating the ROC curve out of a database including dental codes is shown.

5.1 Introduction

The aim of a dental biometric identification method is to automatically analyze dental radiographs (DRs) by comparing unlabeled post-mortem (PM) radiographs acquired after death, against labeled ante-mortem (AM) radiographs acquired before death and stored in a database. The objective of the proposed work is to implement a biometric identification method based on dental works (DWs) information. The algorithm was implemented in Matlab™ and works on panoramic dental radiographs (see chapter 3.4). To achieve comparable conditions which are needed for the matching stage, the dental radiographs (DRs) are registrated, before they are used for further processing.

The proposed method consists of three main processing stages:

1. **Feature extraction:** pre-processing of the DRs and segmentation of the DWs in the DRs.
2. **Dental code generation:** creation of a dental code (DC) out of the information of the detected DWs in the feature extraction stage. The DC includes information about (i) the position (upper or lower jaw), (ii) the size and (iii) the distance between two neighbor DWs.
3. **Matching** of a particular DC with other DCs stored in a database to find out the highest score of similarity.

5.2 Image Registration

The proposed method uses registrated DRs. This is necessary because the DC is generated out of DW information such as the size and the distance between two neighbor DWs. To match two or more different radiographs this information has to be comparable. The DRs in the database do not have the same resolutions (see Fig. 5.1) before registration which means that the same DWs in two different DRs do not have the same size and also the distances differ from each other. The DR is cut because all of the image information of the panoramic DRs is needed.

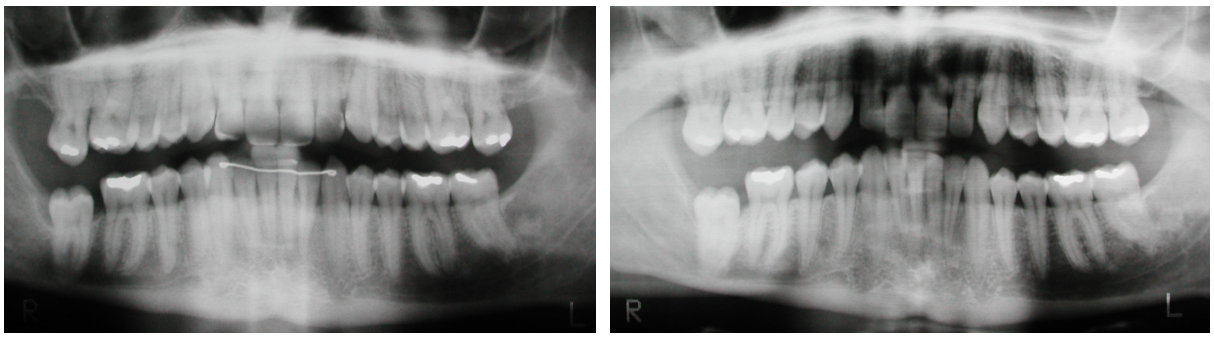

(a) (b)

Figure 5.1: Two AM dental radiographs of the same person (genuine) before registration. The resolutions of the DRs differ from each other and the contrast varies strongly. (a) Acquired in the year 2000, resolution: 1330x738 pixels; (b) Acquired in the year 2003, resolution: 1370x753 pixels.

5.2.1 Manual Image Registration

As mentioned before, to achieve comparable conditions, the dental radiograph (DR) is manually registrated before it is used for further processing. DRs do not include special features, such as markers which could be used for an automatical image registration. To perform the registration, distinctive image features in the DRs are marked manually. These features include the area between the maxillary and the mandibular teeth (position one), and the inside borders of the mandibular (position two and three) which can be seen clearly in each DR, see Fig. 5.2.

After marking all three positions, the image is cut (I_{DR}). The new width (w_{new}) of I_{DR} represents the length between the x-components of the positions two ($x_{position2}$) and three ($x_{position3}$) in the DR. The new height (h_{new}) of I_{DR} is calculated out of w_{new} with an amount of 30%, see Fig 5.2.

$$\begin{aligned} w_{new} &= x_{position3} - x_{position2} \\ h_{new} &= 0.3 \cdot w_{new} \end{aligned} \tag{5.1}$$

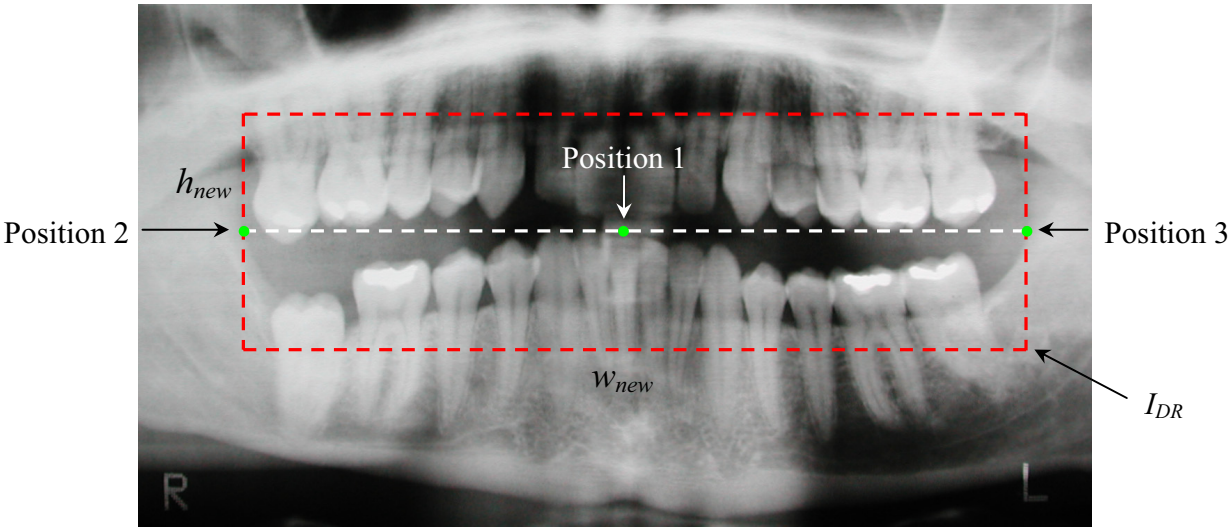

Figure 5.2: Process of image registration. Three positions are marked manually: position 1 represents the area between the maxillary and the mandibular teeth. Position 2 and 3 represent the inside borders of the mandibular. The cut image (I_{DR}) is the area within the rectangle and includes only needed image information such as maxillary and the mandibular teeth.

I_{DR} is resized to a width of 1000 pixels and a height of 300 pixels by using nearest-neighbor interpolation. Nearest-neighbor interpolation is the process of choosing the amplitude of an output image pixel to be the amplitude of the input pixel nearest to the reverse address [42]. Finally, all registrated images have the same resolution which means, that distances and sizes in pixels of different DRs are comparable. Examples of two registrated DRs can be seen in Fig. 5.3.

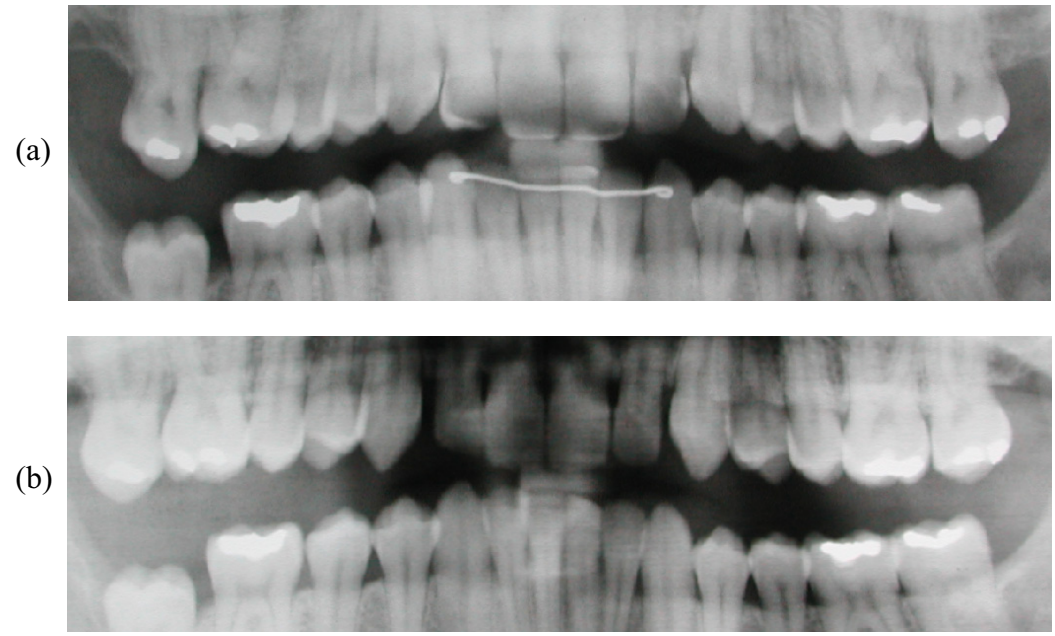

Figure 5.3: Registrated DRs from Fig. 5.1. Both images have a resolution of 1000x300 pixels and include only useful image information (maxillary and the mandibular teeth).

5.3 Processing Stages

The proposed method consists of three main processing stages: feature extraction, creation of a dental code and feature matching, which are now described in detail.

5.3.1 Feature Extraction

The DR is pre-processed to improve the segmentation result:

Median Filtering

To reduce the influence of noise and to achieve better thresholding results, 6x6 median filtering is performed, see Fig. 5.4. The median is defined by the middle value of the given values in their ascending order. When the amount of values is even, the median is the average value of the two middle values. The median filter replaces the value of a pixel by the median of the gray levels in the m-by-n neighborhood around a pixel [37]

$$\widehat{f}(x,y) = \underset{(s,t)\in S_{xy}}{median}\{f(s,t)\} \tag{5.2}$$

whereby S_{xy} represents the set of coordinates in a rectangular subimage $f(s,t)$ of size m x n, centered at point (x,y) and $\widehat{f}$ represents the restored image.

Median filters are quite popular because they provide excellent noise-reduction capabilities with considerable less blurring than linear smoothing filters of similar size. They are very effective when the goal is to simultaneously reduce noise and preserve edges.

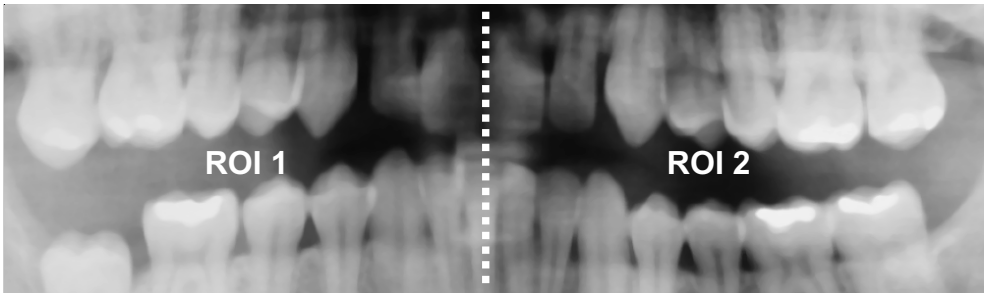

Figure 5.4: Image I_{DR} (b) in Fig. 5.3 after performing median filtering (size 6x6). The image is divided into two ROIs, because of different lightning conditions in the DR.

Different lighting conditions in the DRs may influence the thresholding process. To avoid this problem, the image is subdivided into two regions of interest (ROIs) and local thresholding for each ROI is performed, see Fig. 5.4.

Segmentation - Thresholding

To separate the useful features (DWs) from the background in I_{DR}, an algorithm is used which determines a gray value threshold in the left and the right ROI in I_{DR}. The gray-scale histogram of I_{DR} is used to detect the threshold. The histogram of a digital image with gray levels in the range [0, L-1] is a discrete function $h(r_k) = n_k$, where r_k is the k-th gray level and n_k is the number of pixels in the image having gray level r_k [37]. Typically, the DWs feature the highest intensities in the image and appear as a distinct, relatively small but pronounced mode in the upper range of the histogram, see Fig. 5.5. The algorithm detects the first valley from the right site in the upper range of the histogram. The normal histogram cannot be used because a lot of small valleys are present. To find only the pronounced mode, the histogram is smoothed using a moving average filter. A moving average filter operates by averaging M-points from the input signal to produce each point in the output signal.

$$h_{av}(r_k) = \frac{1}{M} \cdot \sum_{j=-\frac{M}{2}}^{+\frac{M}{2}} h(r_k - j) \tag{5.3}$$

$h(r_k)$ represents the input and $h_{av}(r_k)$ the calculated output histogram using a moving average filter. M is the number of points used in the moving average. The best results for

the smoothed histogram were achieved with a moving average of 5 points (M=5). After smoothing, the threshold is set to the gray-value at the location of the left valley at the rightmost mode which indicates the DWs, see Fig. 5.5.

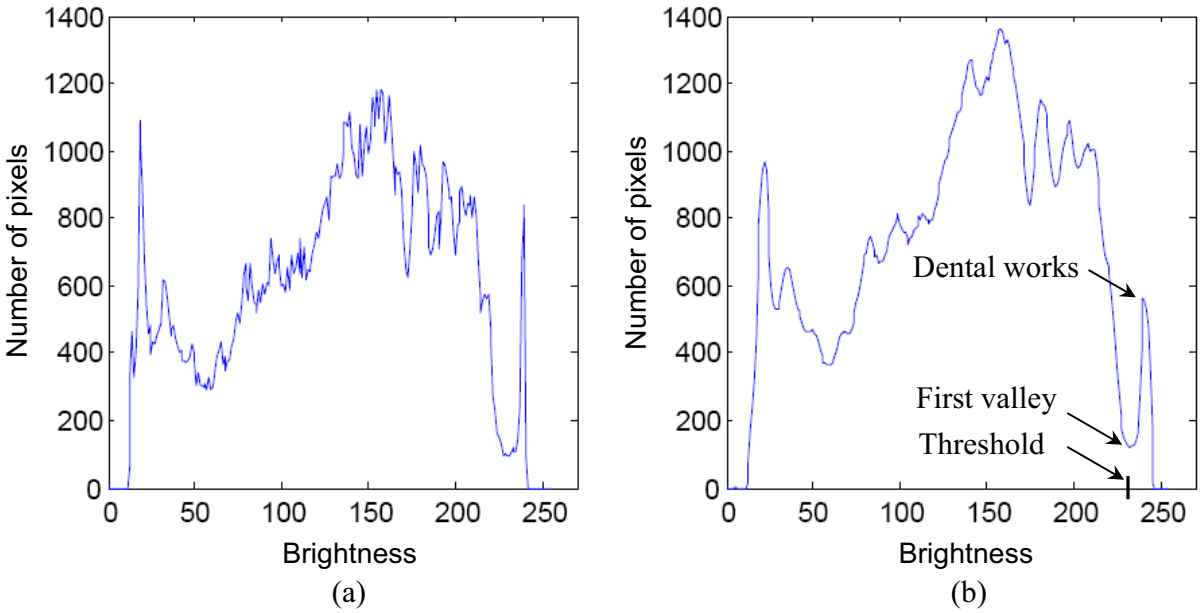

Figure 5.5: Histogram of the ROI 2 in image Fig. 5.4 (a) Before smoothing and (b) after smoothing using a moving average filter (M=5). The detected threshold is set to the gray-value at the location of the left valley at the rightmost mode, which indicates the DWs. In that case, the threshold value is determined to 232.

In some cases a more useful valley in a defined neighborhood (k positions) of the detected threshold (t) is present, see Fig. 5.6. Therefore, the local minimum within k positions of t is detected which represent the new threshold (t_{new}). The best results for k are achieved with 5 (k=5).

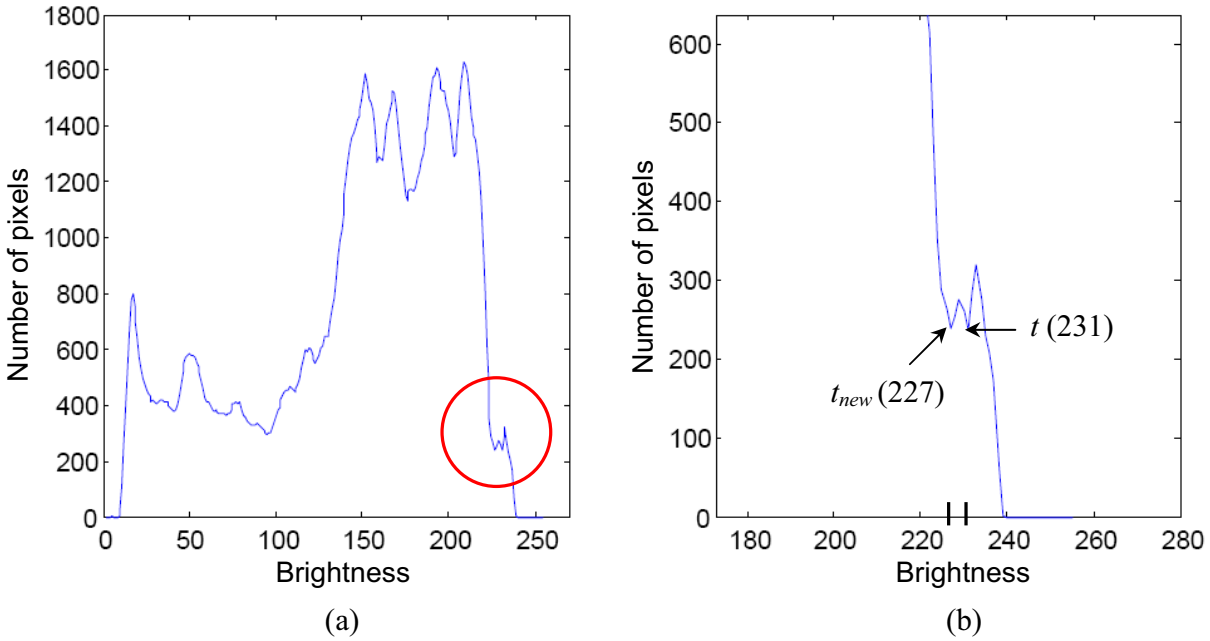

Figure 5.6: Histogram of the ROI 1 in image Fig. 5.4. (a) After smoothing using a moving average filter (M=5). (b) Close-up of the circled area in (a): A better threshold t_{new} (227) than the detected threshold t (231) is found in a defined neighborhood (k=5).

The detected threshold is used to binarize the gray-value image where each region represents a possible DW, see Fig. 5.7.

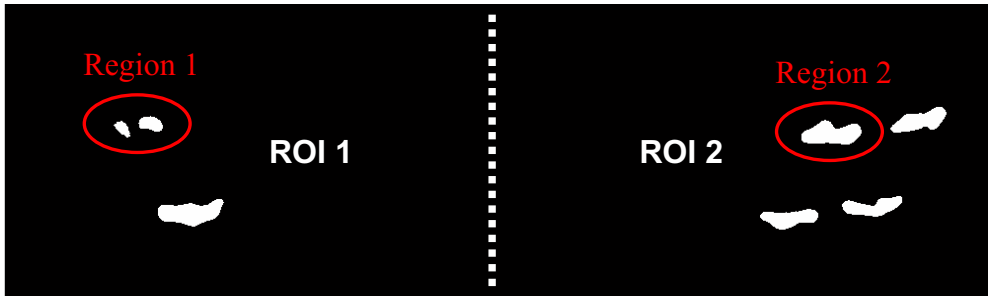

Figure 5.7: Binary mask of the ROI 1 and ROI 2 in Fig. 5.4, including possible dental work regions, e.g. region 1 and region 2.

Improving of the rough segmentation result by applying a Snake

Using only thresholding is not sufficient when working with DRs. In some cases, areas of the DWs which have a lower threshold than the rest of the DW may not be detected which means that the segmentation result is not exact. Therefore, an additional segmentation method called snakes (see chapter 4.1) is used to improve the segmentation result of the DWs. A snake needs to be initialized with an initial closed curve (e.g. a circle) and is an

iterative procedure which stops after a defined number of iterations. The better the initialization curve, the better the performance of the algorithm and the final segmentation result.

Each DW is segmented with a separate snake. Therefore, a subimage I_{DW} for each DW is cut of I_{DR}. To increase the capture range of the snake, the size of I_{DW} is four times bigger than the bounding box for each DW in the binary mask, see Fig. 5.8.

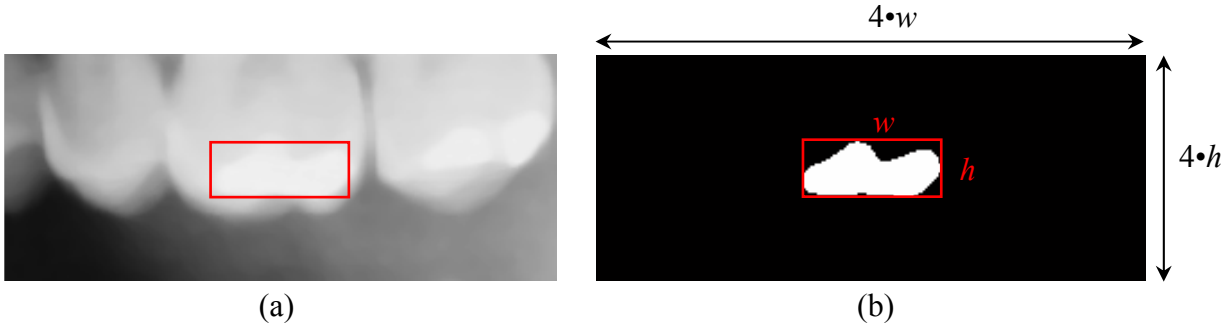

Figure 5.8: Cut subimage I_{DW} (a) for region 2 in Fig. 5.4. The size of I_{DW} is four times bigger than the bounding box (red rectangle) for each DW in the binary mask. (b) Binary mask of I_{DW}.

The external force field (GVF) for the snake is computed out of the gradient image of the edge map of I_{DW}. The edge map is produced by performing a canny edge-detector onto the gray-scale image I_{DW}. An enhanced edge map leads to better segmentation results of the snake. To improve the results of the edge map, gamma correction is used. This process corrects the luminance values in an image by correcting the nonlinear power-law

$$s = cr^{\gamma} \tag{5.4}$$

where c is a constant, r is the input and s the corrected output gray levels. The best results for computing the edge map were achieved with a γ-value of 2 and c-value of 1, see Fig. 5.9. Using gamma correction, more DWs are correctly segmented because additional edge information is given in the edge map. An example of a segmentation enhancement after gamma correction is shown in Fig. 5.10.

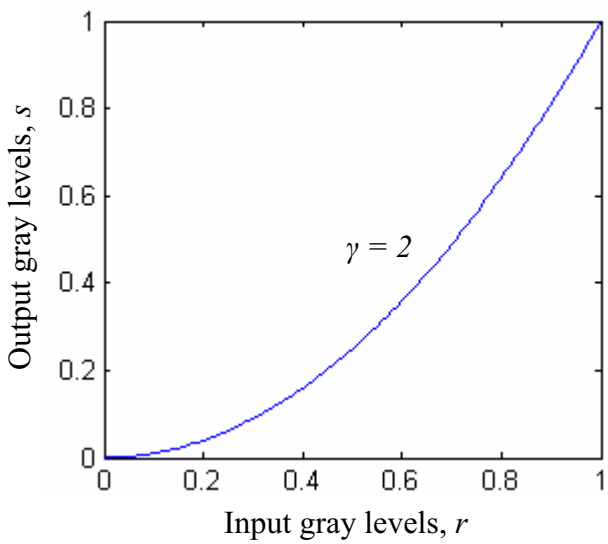

Figure 5.9: Gamma correction: Plot of the power law equation $s = cr^{\gamma}$ for normalized gray levels (c = 1, $\gamma = 2$).

To improve the segmentation and to speed up the algorithm, the initial curves for all DWs are computed from the binary mask. The borders of the detected regions are used as initial curves, see Fig. 5.11(a) and Fig. 5.11(b). The evaluation of the segmentation process of a snake is shown in Fig. 5.11.

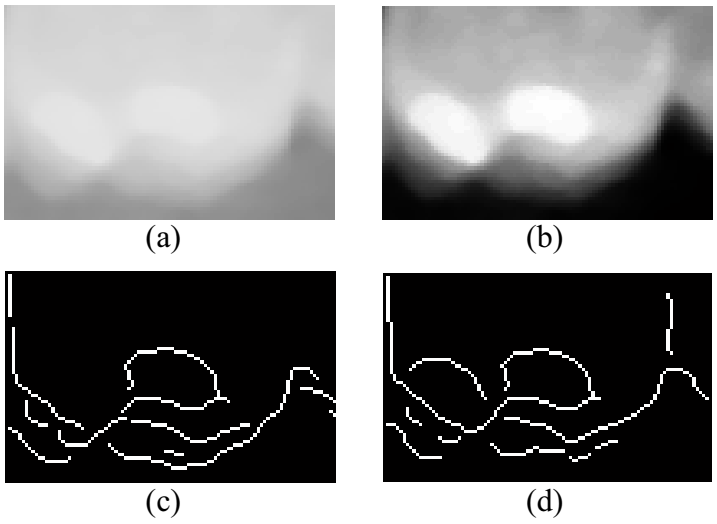

Figure 5.10: Gamma correction for region 1 in Fig. 5.4, using the power-law equation visualized in Fig 5.9. (a) Gray-scale image before and (b) after gamma correction. (c) Edge map of the image in (a) before gamma correction. (d) Enhanced edge map of the image in (b) after gamma correction.

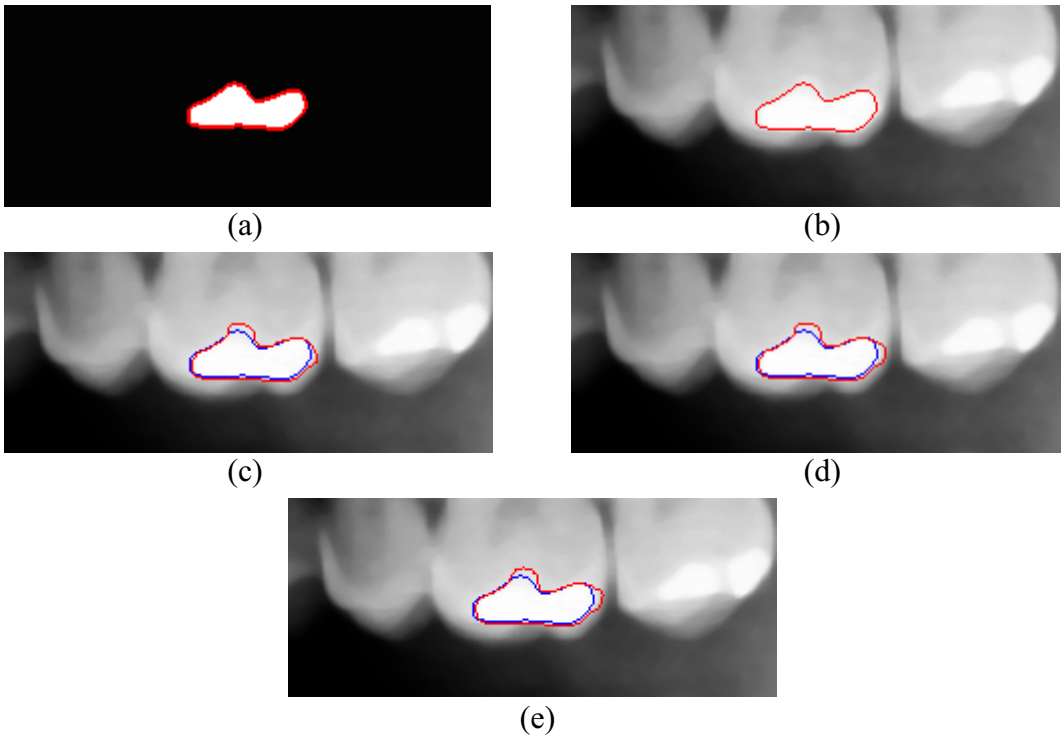

Figure 5.11: Evaluation of the segmentation process of a snake of region 1 in Fig. 5.4. (a) Initial curve in the binary image of I_{DW}, (b) initial curve in I_{DW}, (c) curve transformation after 1 iteration (red curve). The initial curve is shown in blue. (d) Curve transformation after 3 iterations. (e) Final segmentation result after 30 iterations (red curve).

Manually Post-Processing

According to bad segmentation results, like over-segmentation or under-segmentation, different manually post-processing methods have to be used. To improve the performance of segmentation algorithm, further manually post-processing is needed to handle the three different types of errors:

- **Error 1:** In cases of under-segmentation, where DWs are present, but not detected from the algorithm. Therefore, a ROI, in which a DW is present, is selected manually in I_{DW}. The new subimage is called I_{ROI}. To detect the DWs in I_{ROI}, the same segmentation steps as mentioned above for ROI 1 and ROI 2 in I_{DR} are processed. New detected DWs are finally included to the segmentation result of I_{DR}, see Fig. 5.12.
- **Error 2:** In cases of over-segmentation, where regions which do not include DWs are segmented in the DR. This happens in DRs, where DWs do not have a significant higher intensity value than other image structures. Therefore, a manually ROI is selected in which all segmentation results in the binary mask are deleted.
- **Error 3:** In cases, where two or more DWs are connected in the binary mask. This happens because of the smoothing process in the pre-processing stage or in cases,

where needed edges for the snake algorithm could not be detected. Therefore, the connected DWs are separated by manually defining a border between them (polynomial area), see Fig. 5.12.

Final Segmentation Result

A binary mask of the I_{DR} including all automatically and manually detected DWs is created, which is called dental works mask (DWM), see Fig. 5.13.

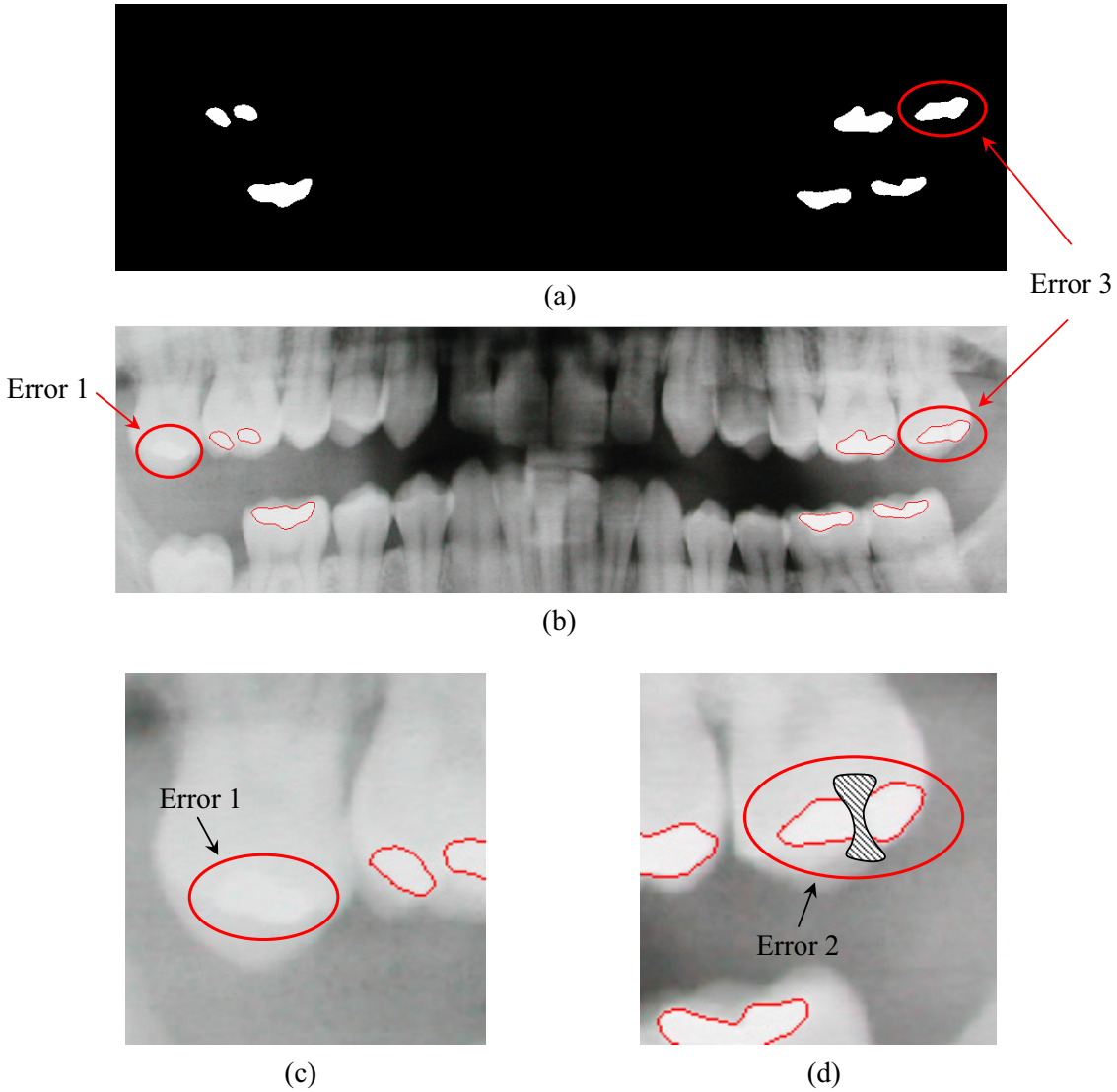

Figure 5.12: Segmentation result before manually post-processing is performed: (a) Binary mask of I_{DR} in (b). (b) I_{DR} including all automatically detected DWs. Error 1: Not detected DW because of under-segmentation. Error 3: Two connected DWs which appear as one. (c) Close-up of Error 1. (d) Close-up of Error 2 including a manually defined polynomial area to separate two connected DWs.

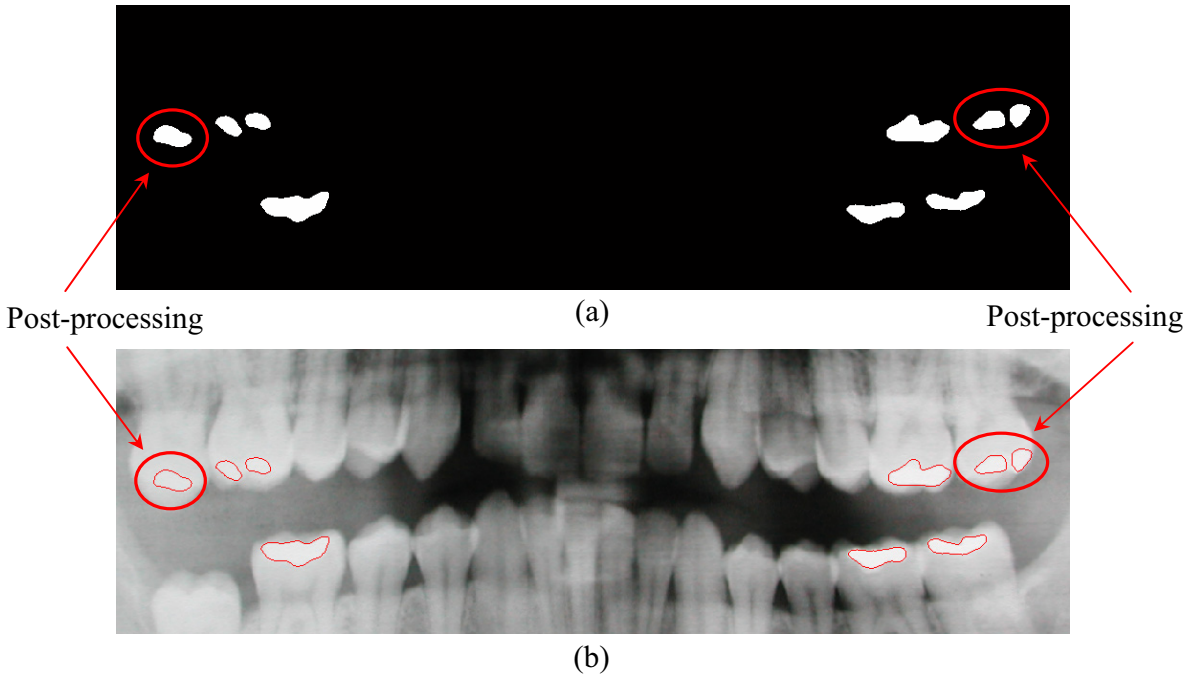

Figure 5.13: Final segmentation result after manually post-processing: (a) DWM of I_{DR} in (b) including all detected DWs. (b) I_{DR} including all detected DWs.

5.3.2 Dental Code Generation

Based on the DWM, a dental code (DC) is created. The DC incorporates information about the detected DWs including position (upper or lower jaw), size and distance between neighboring DWs.

Position of the Dental Works

An algorithm was implemented to sort all DWs in the DWM from left to right based on the center of mass point of each individual DW, see Fig. 5.14.

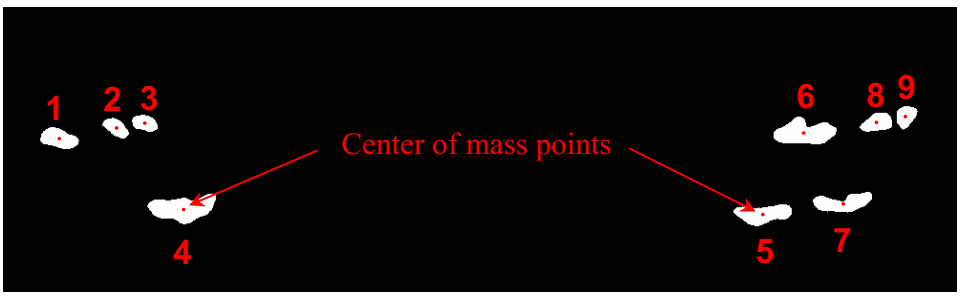

Figure 5.14: DWM with sorted DWs from left to right based on the center of mass point of each individual DW.

For the DC it is also important whether the tooth where the DW is located belongs to the maxilla (upper jaw) or to the mandible (lower jaw). Therefore, a border between the maxilla and the mandible teeth has to be detected. A subimage I_{stripe} is taken out of I_{DR} with the width of the current DW in the DWM. Next, an integral projection on the y-axis is calculated by summing up the intensities of all pixels for each horizontal row in I_{stripe}. The highest intensity represents the area of the DW, see Fig. 5.15. The algorithm detects the first valley on the left and on the right site of the highest intensity point. The valley with the lower intensity represents the border between the maxilla and the mandible teeth. If the position of this valley is above the DW in the image, the DW belongs to the mandible ("L"). If the position is below the DW, the DW belongs to the maxilla ("U"), see Fig. 5.15. The position of the DW is represented in the DC with the letter "L" or "U".

Letter "L" ... DW belongs to a mandibular tooth
Letter "U" ... DW belongs to a maxillary tooth

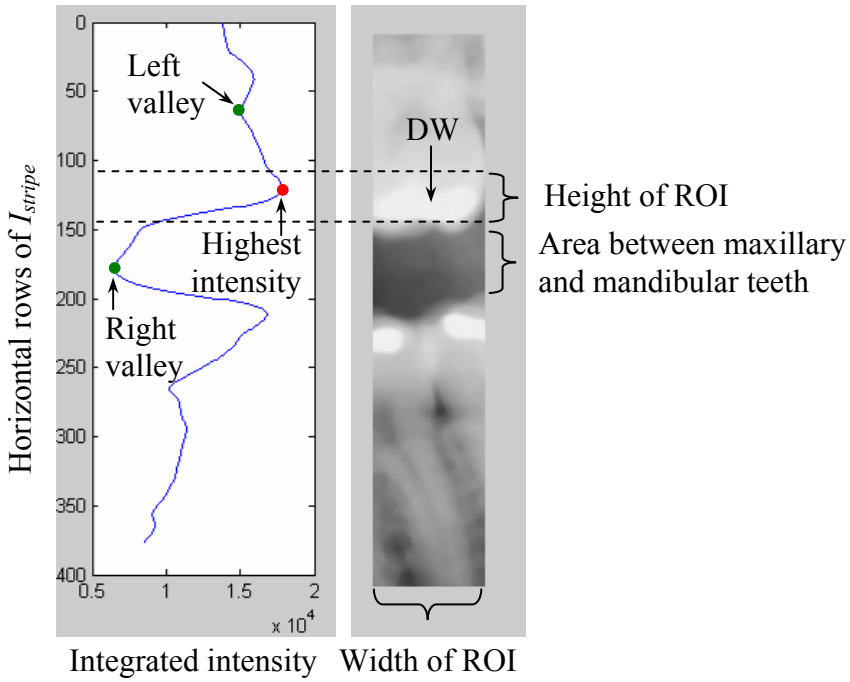

Figure 5.15: Integral projection of a subimage I_{stripe} for region 2 in Fig. 5.7. The width of I_{stripe} equals the width of the DW in the DWM. The right valley represents lower intensity which indicates that the DW belongs to a maxillary tooth. The used symbol in the dental code for this DW is "U".

Size of the Dental Work

The proposed method uses registrated DRs, (see chapter 5.2) which have a size of 1000x300 pixels. According to this, the amount of pixels in a DR is always the same, $A_{total} = 300.000$ pixels. The area A_{DW} of a DW is related to the total image size A_{total}, which results in

the relative area measure for the DW ($A_{DW,rel}$)

$$A_{DW,rel} = \frac{A_{DW}}{A_{total}} \cdot 10^3 \tag{5.5}$$

that is finally used in the DC. To have a better overview in the DC, the $A_{DW,rel}$ is multiplied by 10^3, see Fig. 5.17.

Distance between two neighbor Dental Works

To make the matching algorithm more sensitive, the distance between neighbor DWs is included into the DC. The distance is defined by the amount of pixels between the center of mass points of two DWs. The distance of the leftmost DW (*d1*) is set to zero because no left neighbor DW is present and to make the algorithm more stable against small deviations in the registration of the DRs, see Fig. 5.16. The value for the distance d_{DW} is given in percentage of the total width d_{total} of the DR, which is always 1000 pixels.

$$d_{DW} = \frac{dx}{d_{total}} \cdot 10^2, \quad x = 1..8 \tag{5.6}$$

To have a better overview in the DC, the distance is multiplied by 10^2, see Fig. 5.17.

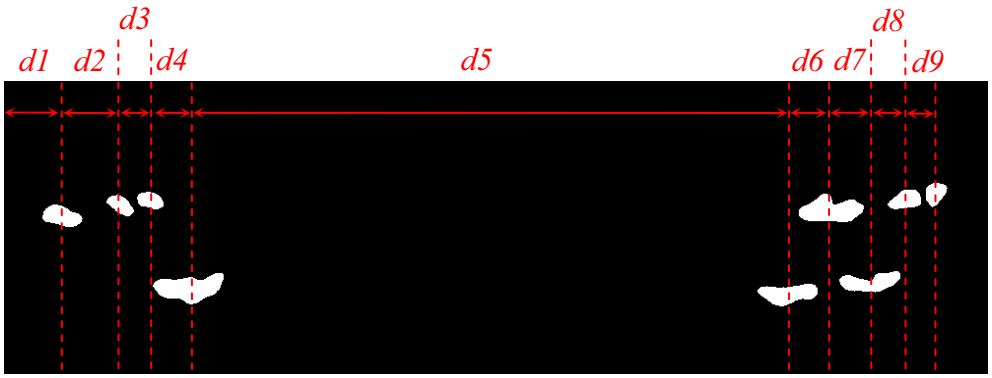

Figure 5.16: Distances (*d1-d9*) between two neighbor DWs in the DWM. The distances of the leftmost DW (*d1*) is set to zero because no left neighbor DW is present and to make the algorithm more stable against small deviations in the registration of the DRs.

From this information, the DC is built of the following three characteristics: (i) the position of the DW ("L" or "U"). (ii) the size of the DWs, and (iii) the distance between two neighboring DWs, see Fig. 5.17.

$$DC = \underbrace{(Position, Size, Distance)\_}_{1.DW}\underbrace{(Position, Size, Distance)\_}_{2.DW}$$

$$DW = [U, L]A_{DW} - d_{DW}\_$$

DC = "U2.1-0_U1.207-6_U1.187-3_L4.773-3.9_L3.063-60.6_U3.893-4.4_L2.86-4_U3.093-4.9_"

Figure 5.17: Final DC for a DR.

5.3.3 Matching

After the DC is created, it can be compared to other DCs in a database. These can be different codes of the same person (genuine matching) or codes of different persons (impostor matching). An algorithm was implemented which uses the Levenshtein distance (Edit distance) for the matching process, see chapter 4.2. Because of the structure of the DC, it was necessary to adapt the original algorithm of the Levenshtein distance. Not only the position (letters "U" and "L)" for each DW have to be compared, but also the size and the distance between neighbor DWs.

The costs of the insertion, deletion, or substitution operations, which are needed to calculate the Levenshtein distance, were tuned in order to obtain the optimal matching performance by testing the algorithm. In the case of insertion and deletion, the matching cost is 60, see Tab. 5.1. In the case of substitution, the cost for comparing two DWs is given by the sum of two costs:

1. The cost of comparing the size of two DWs
2. The cost of comparing the distance of two DWs.

Cost for comparing the Size of two DWs

If the sizes of the compared DWs differ more the 100%, the cost is set to 20. In the other case, the cost for comparing the size is set according to the percentage difference of the compared DWs, see Tab. 5.1.

Cost for comparing the Distances of two DWs

If the distance between the compared DWs differs more than 15%, the cost is set to 20. In the other case, the cost for comparing the distances is set according to the percentage difference of the compared DWs, see Tab. 5.1.

Table 5.1: Costs for insertion, deletion and substitution which are used to calculate the the Levenshtein distance.

Operation	**Matching cost**
insertion	60
deletion	60
substitution	*Comparing the size:* 0, difference between 0..10% 1, difference between 10..20% ... 10, difference between 90..100% 20, difference > 100% *Comparing the distance:* 0, difference between 0..1% 1, difference between 1..2% ... 15, difference between 14..15% 20, difference > 15%

Chapter 6

Results

The following chapter provides the results of the proposed dental biometric method. The robustness of the segmentation method in respect to additive white Gaussian noise and Gaussian blurring is evaluated and ROC curves for size and distance matching of the DWs is created. Finally, the accuracy curve of retrieving subjects from the database is shown.

6.1 Introduction

In order to make a statement about the performance of the proposed method, various tests have been performed. A stable segmentation stage is important for the method because the DC for the matching stage is created out of the results of the segmentation methods. The first testing stage tests the robustness of the segmentation method against influences added to the DRs, such as white Gaussian noise and Gaussian blurring.

To compare biometric methods, the ROC and the accuracy curve are used. In the second testing stage, the matching performance was tested in detail by creating ROC curves for size matching, distance matching and a combination of both followed by creating an accuracy curve to test the subject's retrieval performance.

6.1.1 Robustness of the Segmentation Method

To test the method against influences such as white Gaussian noise and Gaussian blurring, five DRs are chosen which need a minimum of human intervention before the influences were added onto the DRs, see Fig. 6.1. To obtain comparable results, DWs such as braces are not included to the segmentation results because they are not permanently present, see Fig 6.1. The number of manually post-processing steps, according to the three different error types (see chapter 5.3.1), is listed in Tab. 6.1 and divided into the following categories: error 1 (under-segmentation), error 2 (over-segmentation) and error 3 (connected DWs).

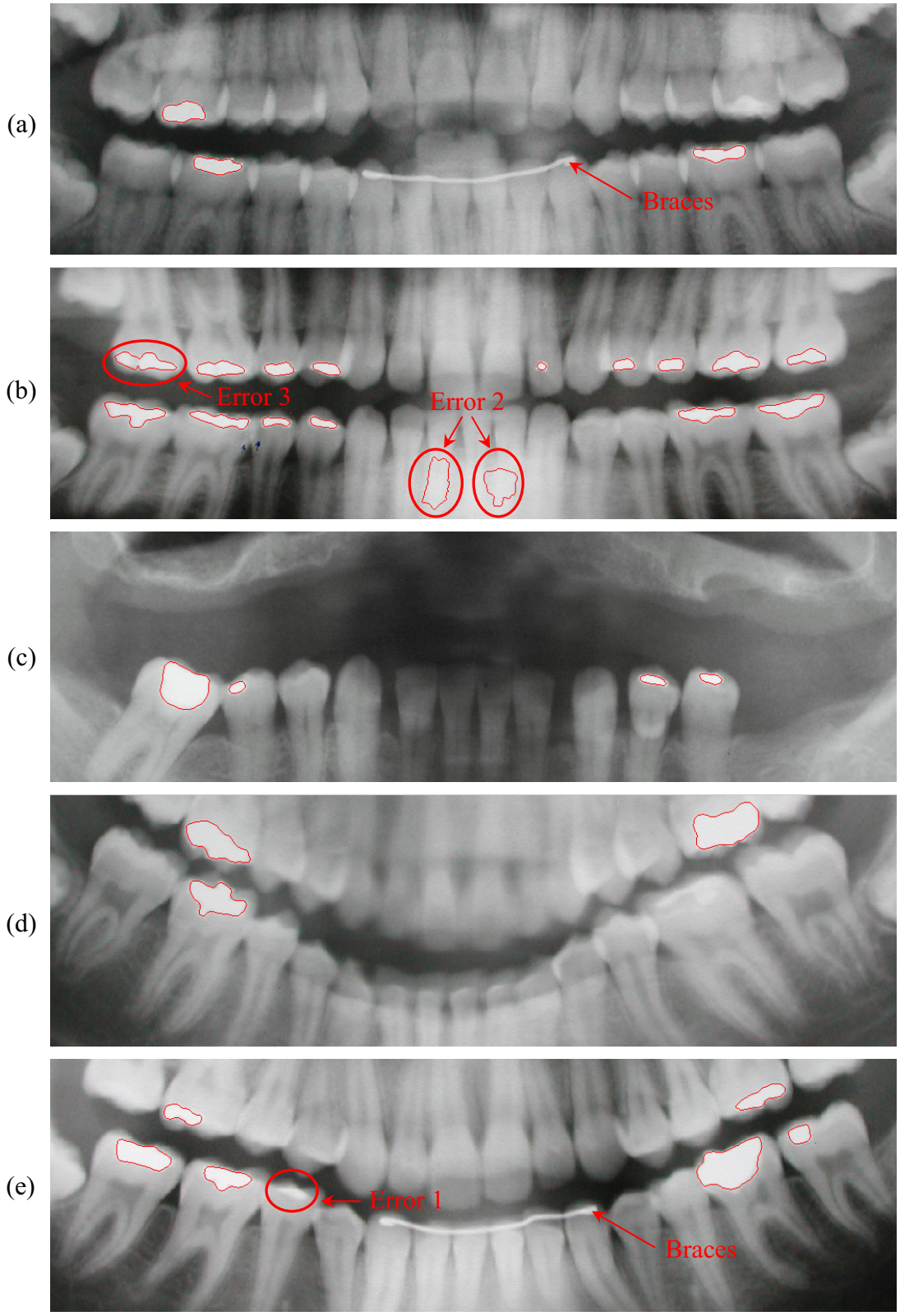

Figure 6.1: Segmentation results of the five used DRs (a-e). Locations, where manually post-processing would be needed are marked with circles and labeled with the occurred error type. Error 1 (under-segmentation), error 2 (over-segmentation) and error 3 (connected DWs). Braces in the DRs (a) and (b) are not included to the segmentation results.

Table 6.1: Amount of segmentation errors before image influences are added. Error 1 (under-segmentation), error 2 (over-segmentation) and error 3 (connected DWs).

DR	**Error** 1	**Error** 2	**Error** 3
a	-	-	-
b	-	2	1
c	-	-	-
d	-	-	-
e	1	-	-

Cases of detecting DWs but not segmenting the whole DW areas correctly are also treated as errors. This occurs if only a part of the DW area (under-segmentation) or an area larger than the DW area (over-segmentation) is segmented, see Fig. 6.2.

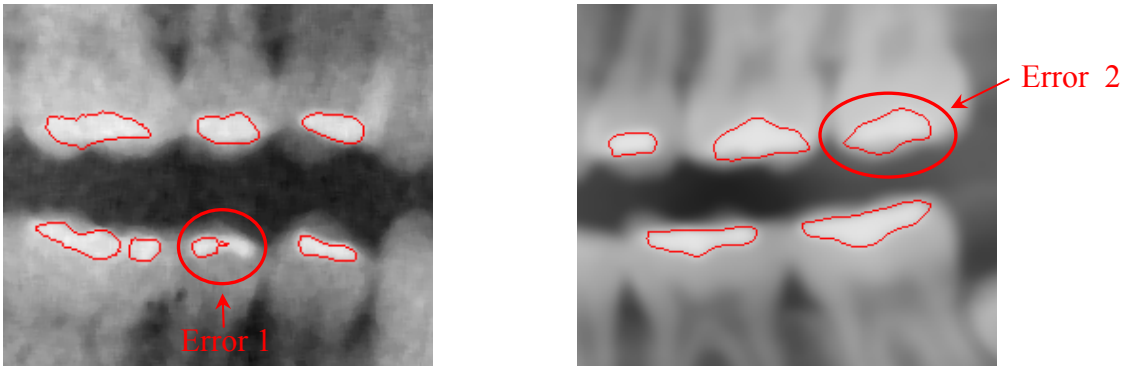

Figure 6.2: Segmentation errors. (a) Close-up of the DR shown in Fig. 6.1(a) after white Gaussian noise is added (CNR = 20dB). Error 1 (under-segmentation): the entire DW area is not segmented correctly. (b) Close-up of the DR shown in Fig. 6.1(b) after Gaussian blurring is performed. $\sigma = 3$, filter size = 20 x 20. Error 2 (over-segmentation): An area larger than the DW area is segmented.

6.1.2 Image Noise

To test the robustness of the segmentation method in the presence of white Gaussian noise with variance (σ_n^2) is added to the DRs using three different contrast noise ratios (CNR), see Fig. 6.3.

The CNR is defined as

$$CNR = 20 \cdot \log \frac{c}{\sigma_n} \tag{6.1}$$

where $c = \max(f(x)) - \min(f(x))$ is the contrast in the image and σ_n is the standard deviation of the noise. The CNR values have to be constant for all tested images to obtain comparable results. This means that the variance (σ_n^2) of the noise have to be determined for each tested image according to:

$$\sigma_n^2 = \frac{c^2}{10^{\frac{CNR}{10}}} \tag{6.2}$$

The changes in the segmentation results after adding certain noise levels to the DR are shown in Tab. 6.2.

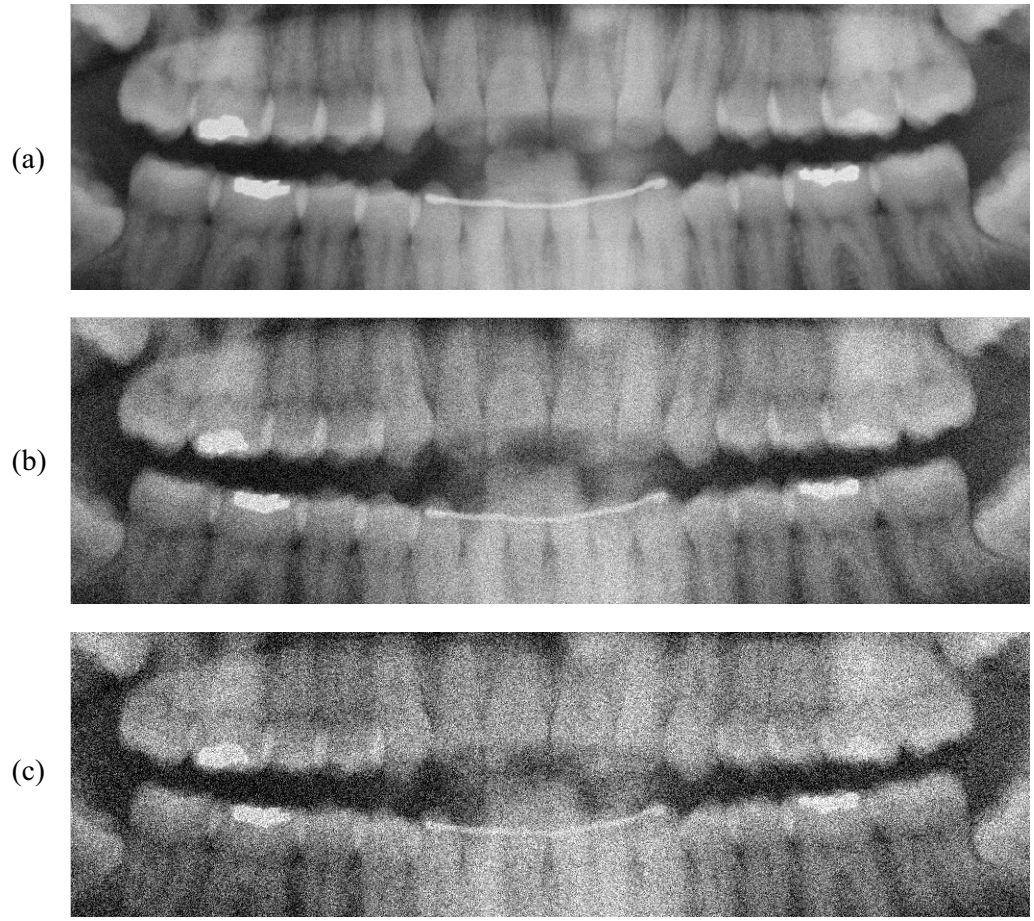

Figure 6.3: DR shown in Fig. 6.1(a) after white Gaussian noise is added. (a) CNR = 30dB, (b) CNR = 20dB and (c) CNR = 15dB.

Table 6.2: Amount of segmentation errors after white Gaussian noise is added to the DRs. Error 1 (under-segmentation), error 2 (over-segmentation) and error 3 (connected DWs). The first value represents a CNR of 30dB, the second a CNR of 20dB and the third a CNR of 15dB; (CNR = 30dB/ CNR = 20dB/ CNR = 15dB). The character x represents a non useable segmentation result, see Fig. 6.4.

DR	**Error** 1	**Error** 2	**Error** 3
a	- / 1 / 3	- / - / -	- / - / -
b	2 / 3 / x	1 / 5 / x	- / - / x
c	- / - / 4	- / - / -	- / - / -
d	- / 1 / x	- / 1 / x	- / - / x
e	1 / 7 / x	- / 1 / x	- / - / x

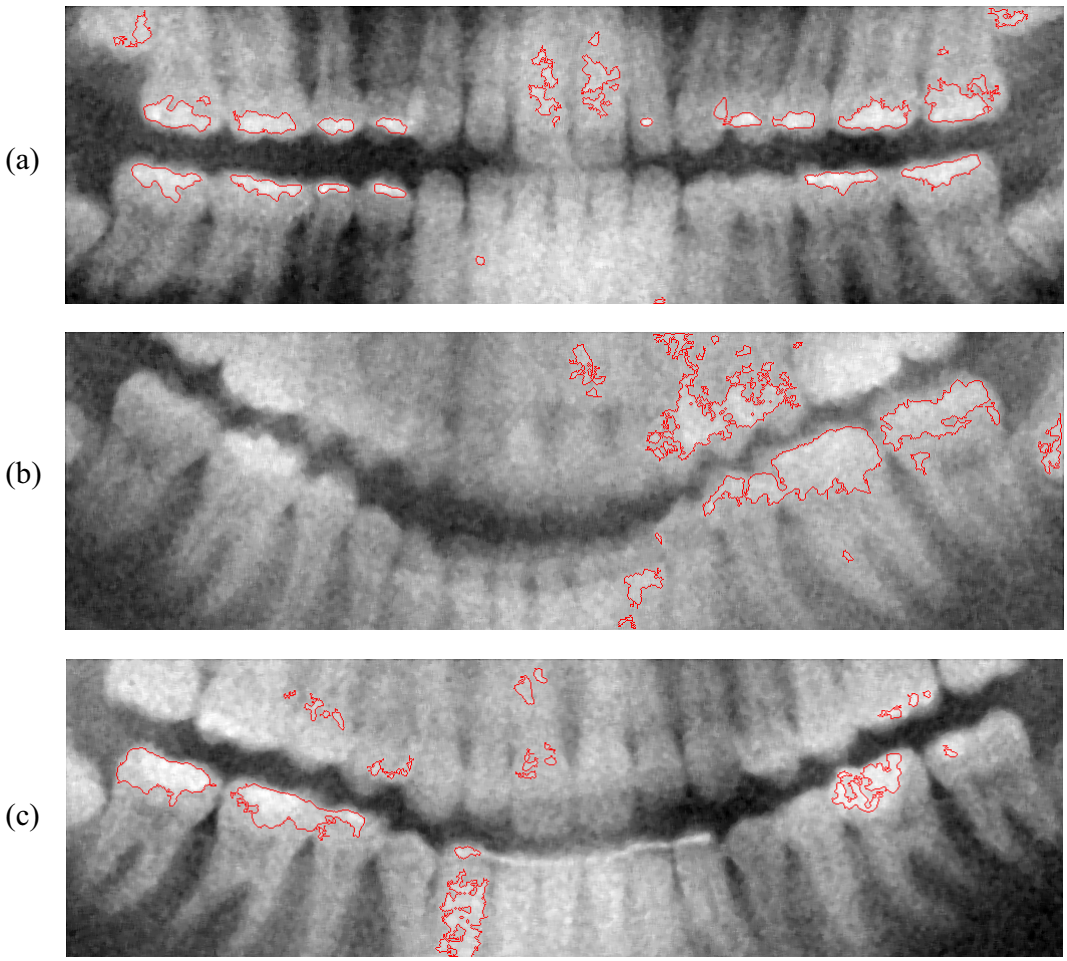

Figure 6.4: DRs shown in Fig. 6.1(b,d,e) after white Gaussian noise (CNR = 15 dB) is added. The segmentation results cannot be used for further processing.

Conclusion:

The stability of the segmentation method against white Gaussian noise was tested by using three different CNR (15dB, 20dB and 30dB). The algorithm is robust to noise up to a CNR of 30dB.

Various errors, especially class 1 errors (under-segmentation), occurred by using a CNR of 20dB and lower. The segmentation results cannot be used for further processing if noise that leads to a CNR of 15dB and lower is added to the DR, see Fig 6.4.

6.1.3 Image Blurring

The segmentation method is tested on blurred DRs. A Gaussian blurring filter is used to simulate out of focus conditions, see Fig. 6.5. The equation of a two-dimensional Gaussian filter is given by:

$$G(x, y) = \frac{1}{2\pi\sigma^2} \cdot e^{-(x^2+y^2)/(2\sigma^2)} \tag{6.3}$$

where $r = \sqrt{x^2 + y^2}$ is the blurring radius, and σ is the standard deviation of the Gaussian kernel. The changes in the segmentation results after performing Gaussian blurring are shown in Tab. 6.3.

Table 6.3: Amount of segmentation errors on Gaussian blurred DRs. Error 1 (under-segmentation), error 2 (over-segmentation) and error 3 (connected DWs). The first value represents the amount of errors according to a σ of 2, the second to a σ of 3 and the third to a σ of 5; ($\sigma = 2$ / $\sigma = 3$ / $\sigma = 5$). The filter size is 20 x 20).

DR	**Error** 1	**Error** 2	**Error** 3
a	- / - / 1	- / - / 1	- / - / -
b	3 / 5 / 9	1 / 4 / 3	- / 1 / -
c	- / 1 / 2	- / - / -	- / - / -
d	- / - / -	- / - / 1	- / - / -
e	1 / 1 / 4	- / - / -	- / - / -

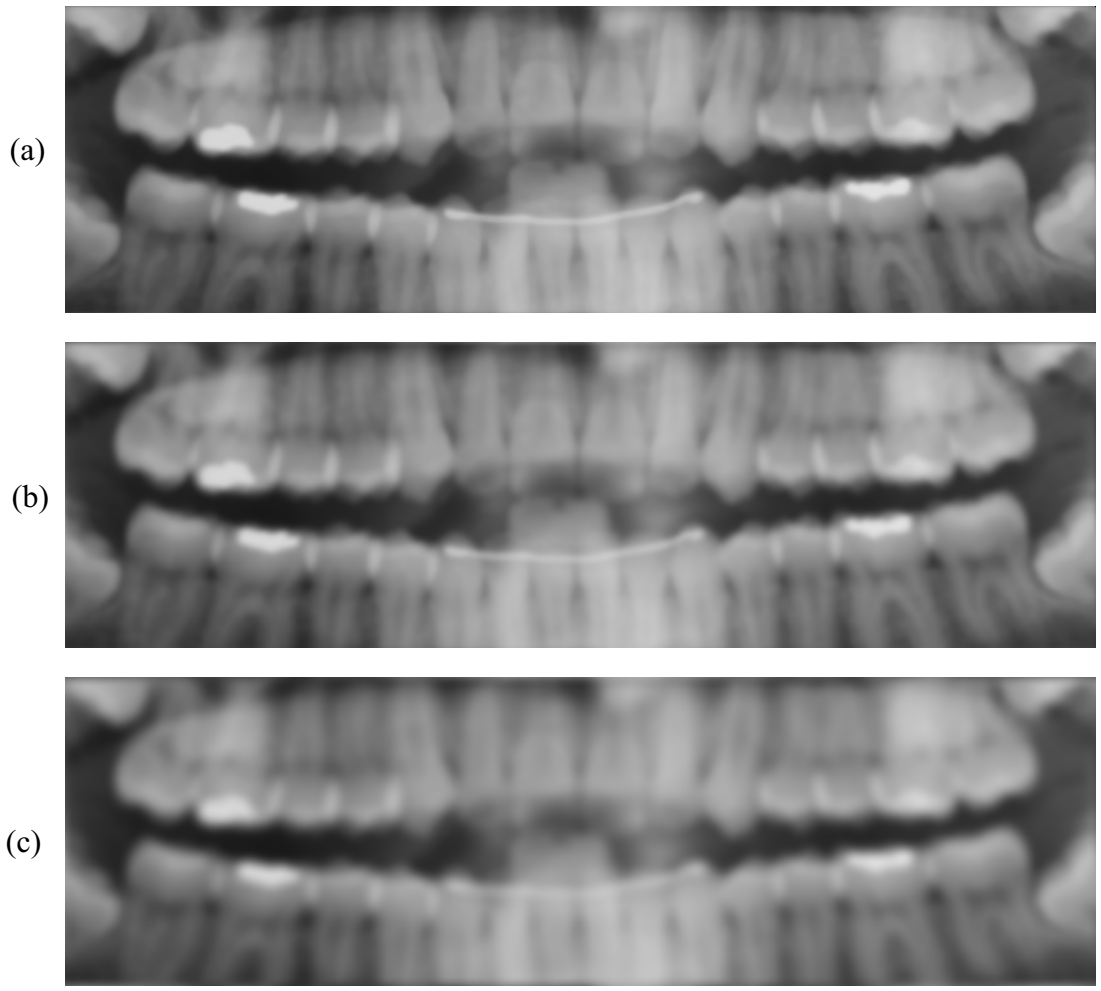

Figure 6.5: DR shown in Fig. 6.1(a) after Gaussian blurring is performed on the DRs. Filter size = 20 x 20, (a) $\sigma = 2$, (b) $\sigma = 3$ and (c) $\sigma = 5$.

Conclusion

The stability of the segmentation method in respect to Gaussian blurring was tested by using three different blurring strengths. Blurring affects the segmentation result in the form of under-segmentation and over-segmentation.

Up to a blurring of $\sigma = 3$ and a filter size of 20 x 20 the segmentation results can be used for further processing. Above this σ-value (e.g. $\sigma = 5$), the amount of class 1 errors increase significantly by as can be seen Tab. 6.3.

6.2 Matching Performance

A database including 68 DRs was used in the experiments to evaluate the proposed dental biometric method: a pair of DRs for 22 subjects (44 DRs) plus a single DR for the other 24 subjects. For the 22 subjects with two DRs, their oldest DRs were considered as AM (ante-mortem) DRs and their newest DRs were considered as PM (post-mortem) DRs. For the 24 subjects with only one DRs, the DRs were considered as AM DRs. This has to be done, because no access to an official DR database including AM and PM DRs is granted. The DRs were manually registrated to obtain comparable conditions, see chapter 5.2. In cases of over-segmentation or under-segmentation of the DWs, the segmentation result had to be corrected manually. Also, if DWs are not detected by thresholding, a ROI has to be selected manually in the DR to perform local thresholding, see chapter 5.3.1.

6.2.1 Size and Distance Matching

The first version of the method included only the size of the detected DWs as information in the DC. Figure 6.6 shows the ROC curve (see chapter 2.5.2) of the matching performance for the proposed method. The ROC curve shows that the method obtained 13.6% of EER. The EER is the value where the FAR is equal to the FRR. The lower the EER, the better is the performance of the biometric system.

Not only the size but also the distance between neighbor DWs in the DR can be used as matching information. The ROC curve shows that an EER of 10.1% is obtained by using only the distance as information in the DC, see Fig. 6.6.

6.2.2 Combination of Size and Distance Matching

To make the matching algorithm more sensitive, the size of the DWs and also the distance between neighbor DWs are included into the DC. Using a combination of this information, the value for the EER improves to 9.8% which is a good result for the used database, see Fig. 6.7.

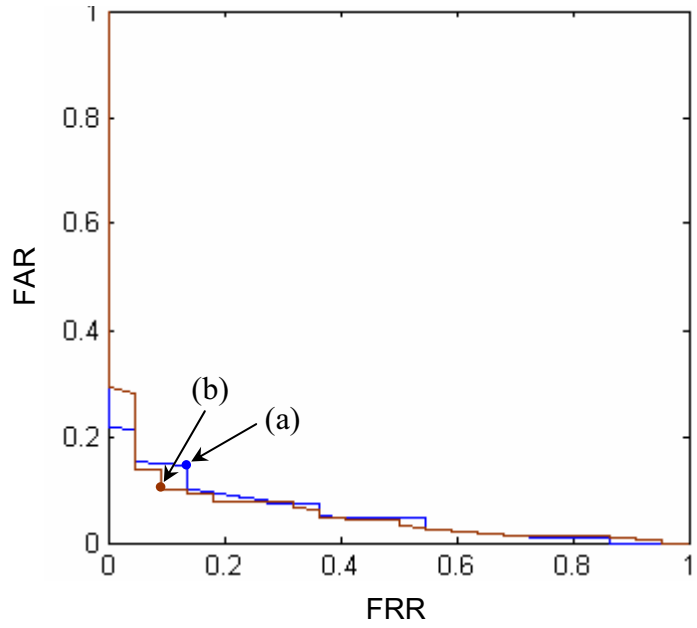

Figure 6.6: ROC curves. (a) EER (13.6%) of matching the size of the DWs and (b) EER (10.1%) of matching the distance between neighbor DWs.

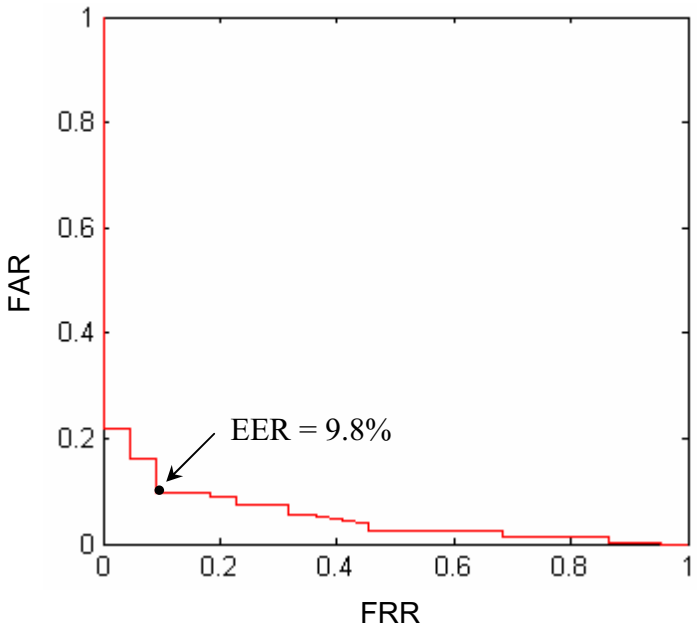

Figure 6.7: Final ROC curve using a combination of size and the distance matching of the detected DWs. EER = 9.8%.

6.2.3 Accuracy Curve

To test the retrieving accuracy, PM DRs are matched against a larger set of AM DRs, including the correct pairs of the PM DRs, see Fig. 6.8.

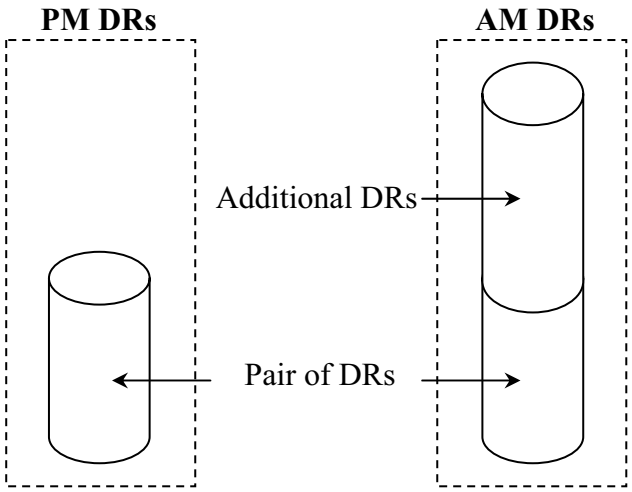

Figure 6.8: Used database scheme for accuracy testing. PM DRs are matched against a larger set of AM DRs including the corresponding pairs of the PM DRs.

Figure 6.9 shows the accuracy curve obtained when the 22 PM DRs were matched to the 46 AM DRs of the database. Top-1 retrieval means that the correct match has highest matching score. Top-2 retrieval means, that the correct match is within the two highest matching scores. Using the top-1 retrieval, the accuracy was 18/22 (= 82%). Using top-2 retrievals, the retrieving accuracy is 91%. The accuracy reaches 100% when the top-11 retrievals are used.

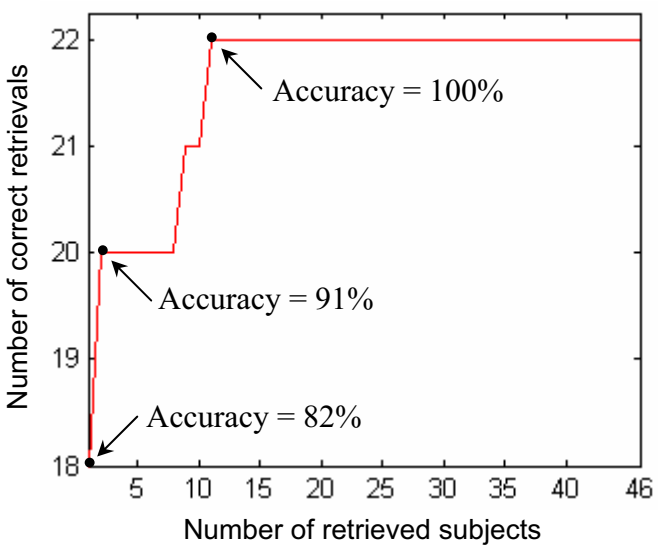

Figure 6.9: Accuracy curve obtained when 22 subjects were identified from 46 possible identities. Using the top-1 retrieval, the accuracy is 82%. Using top-2 retrievals, the retrieving accuracy is 91%. 100% accuracy is reached by using the top-11 retrievals were used.

Chapter 7

Conclusion and Future Work

Biometrics is a relatively new technology, which is being deployed in public and private sector applications and, thus, has received much attention in the last years. Dental biometrics is used in the forensic medicine to identify individuals based on their dental characteristics by comparing unlabeled post-mortem with labeled ante-mortem radiographs.

This work presents a new dental biometric identification method based only on dental work information extracted from panoramic dental radiographs. The proposed method consists of three main stages: (i) feature extraction, where biometric information of the dental works is extracted, (ii) generation of a dental code, and (iii) matching, where the dental codes are compared against dental codes in a database. In the feature extraction stage, seed points of the dental works are detected by thresholding. The final segmentation is obtained by using a snake (active contour) algorithm. The dental code incorporates information about the position (upper or lower jaw), the size of the dental works and the distance between two neighboring dental works. The matching stage works with the Levenshtein distance (Edit distance) whereby the operations substitution, insertion and deletion were adapted to optimize the matching performance.

The database used in the experiments contained 68 DRs, and the obtained matching results were promising especially considering that only dental work information is considered by the method. An equal error rate (EER) of 9.8% and an accuracy of 82% for the top-1 retrieval is achieved. In the experiments, the proposed segmentation method performs accurate segmentation but there are still a number of open challenges. The feature extraction (segmentation of the DWs) is a difficult problem for dental radiographs, especially for poor quality images where some dental work contours are indiscernible. In these cases it is difficult to successfully apply the proposed method. In the cases of over-segmentation or under-segmentation of the DWs, the segmentation results have to be corrected manually.

7.1 Future Work

In future work, a rotation-invariant algorithm will be developed. The DRs will be automatically normalized based on the detection of a middle line between the upper and the lower teeth. Out of this information, image distortions will be corrected automatically. A more accurate normalization should increase the performance of the proposed identification method because the sizes of the DWs and the distances between neighboring DWs are dependent on the size of the DRs.

More comprehensive tests, especially in the feature extraction and matching stage, will be conducted to point out the strengths and the weaknesses of the method more clearly. According to the test results, the algorithm will be adapted to be more robust.

Because the amount of images in the database is low, it is not possible to make a reliable statement about the performance and effectiveness of the proposed method. In future work, the proposed method will be evaluated using a larger database.

Bibliography

[1] EyadHaj Said, Gamal Fahmy, Diaa Nassar, and Hany Ammar. Dental X-ray image segmentation. Technical report, Lane Department of Computer Science and Electrical Engineering, West Virginia University, Morgantown, 2001.

[2] P. O'Shaughnessy. More than half of victims idd. *New York Daily News*, 2002. http://www.nydailynews.com/news/local/story/17949p-17009c.html , Sept. 11, 2002 [Jan. 23, 2007].

[3] Hong Chen and A.K. Jain. Dental biometrics: alignment and matching of dental radiographs. *Pattern Analysis and Machine Intelligence, IEEE Transactions on*, 27(8):1319–1326, Aug. 2005.

[4] Anil K. Jain and Hong Chen. Matching of dental x-ray images for human identication. *Pattern Recognition - The Journal of the pattern recognition society*, 37:1519 – 1532, 2004.

[5] National Science and Technology Council. Biometrics "foundation documents". Subcommittee on Biometrics, http://www.biometrics.gov/docs/biofoundationdocs.pdf, [June 19, 2007].

[6] Sharath Pankanti A.K. Jain, Ruud Bolle, editor. *Biometrics: Personal Identification in Networked Society*. Springer, 1998. ISBN: 0792383451.

[7] T. Mansfield and G. Roethenbaugh. Glossary of biometric terms. Association for Biometrics (AfB) and International Computer Security Association (ICSA). 1999.

[8] H. Gamboaa and A. Fred. A behavioural biometric system based on human computer interaction. 2003.

[9] Herbert Leitold and Reinhard Posch. Leitfaden biometrie: Überblick und stand der technik. Secure Information Technology Center - Austria. 2004.

[10] Arun A. Ross, K. Nandakumar, and Anil K. Jain. *Handbook of Multibiometrics*, volume 6. Springer, 2006. ISBN: 978-0-387-22296-7.

[11] National Science and Technology Council. Biometrics glossary. Subcommittee on Biometrics, http://www.biometrics.gov/docs/glossary.pdf, [June 19, 2007].

[12] Hanna-Kaisa Lammi. Ear biometrics. Lappeenranta University of Technology, Department of Information Technology, Laboratory of Information Processing. 2005.

[13] International Biometrics Group. Is dna a biometric? 2007. http://www.biometricgroup.com/reports/public/reports/dna.html, [June 19, 2007].

[14] ChewYean Yam, Mark S. Nixon, and John N. Carter. Gait recognition by walking and running: A model-based approach. Image, Speech and Intelligent Systems, Electronic and Computer Science University of Southampton. 2002.

[15] J.D. Woodward. Biometrics: privacy's foe or privacy's friend? *Proceedings of the IEEE*, 85(9):1480–1492, Sept. 1997.

[16] National Science and Technology Council. Biometrics testing and statistics. Subcommittee on Biometrics, http://www.biometrics.gov/docs/biotestingandstats.pdf, [June 19, 2007].

[17] HumanScan GmbH. About far, frr, eer. http://www.bioid.com/sdk/docs/About_EER.htm, March 3, 2004 [June 19, 2007].

[18] Gamal Fahmy, Diaa Nassar, Eyad Haj-Said, Hong Chen, Omaima Nomir, Jindan Zhou, Robert Howell, Hany H. Ammar, Mohamed Abdel-Mottaleb, and Anil K. Jain. Towards an automated dental identification system (adis). 2004.

[19] Michael C. Bowers. *Forensic Dental Evidence, An investigators's Handbook*. Academic Press, 2004. ISBN-10: 0-12-121042-1, ISBN-13: 978-0-12-121042-7.

[20] The British Association for Forensic Odontology (BAFO). Forensic odontology. http://www.bafo.org.uk/guide.php, [June 19, 2007].

[21] C. Savio, G. Merlati, P. Danesino, G. Fassina, and P. Menghini. Radiographic evaluation of teeth subjected to high temperatures: Experimental study to aid identification processes. *Forensic Science International*, 158(2):108–116, 2006.

[22] Mary A Bush, Raymond G Miller, Jennifer Prutsman-Pfeiffer, and Peter J Bush. Identification through x-ray fluorescence analysis of dental restorative resin materials: a comprehensive study of noncremated, cremated, and processed-cremated individuals. *J Forensic Sci*, 52(1):157–165, Jan 2007.

[23] SweetHaven Publishing. Fundamentals of dental technology. http://www.waybuilder.net/sweethaven/MedTech/Dental/Dental01/Dental01_v1.asp?file=0205, 2006 [June 19, 2007].

[24] Dental Find Dentist Directory. Restoration. http://www.dentalfind.com/glossary/, [June 19, 2007].

[25] Delta Dental of California. Glossary of dental health terms. http://www.deltadentalca.org/health/dental_terms.html, 2005, [June 19, 2007].

[26] Martin S. Spiller. Dental x-rays. http://www.doctorspiller.com, 2000 [June 19, 2007].

[27] Anil K. Jain and Hong Chen. Registration of dental atlas to radiographs for human identification. *Proceedings of the SPIE*, 5779:292–298, 2005.

[28] American Board of Forensic Odontology. http://www.abfo.org/, June 4, 2007 [June 19, 2007].

[29] M. Mahoor and M. Abdel-Mottaleb. Automatic classification of teeth in bietwing dental images. *International Conference on Image Processing (ICIP)*, 2004.

[30] T. M. Nazmy, F. M. Nabil, D. A. Salam, and H. M. Samy. Dental radiographs matching using morphological and pcnn approach. *Conference on Graphics, Vision and Image Processing (GVIP)*, 2005.

[31] Hong Chen and A.K. Jain. Tooth contour extraction for matching dental radiographs. In *Pattern Recognition, 2004. ICPR 2004. Proceedings of the 17th International Conference on*, volume 3, pages 522–525Vol.3, 23-26 Aug. 2004.

[32] A. K. Jain, S. Minut, and H. Chen. Dental Biometrics: human identification using dental radiographs. *Proceedings of the 4th International Conference on Audio- and Video-Based Biometric Person Authentication*, (0), June 2003.

[33] M. Kass, A. Witkin, and D. Terzopoulos. Snakes: Active contour models. *IJCV*, 1(4):321–331, January 1988.

[34] Chenyang Xu and J.L. Prince. Gradient vector flow: a new external force for snakes. In *Computer Vision and Pattern Recognition, 1997. Proceedings., 1997 IEEE Computer Society Conference on*, pages 66–71, 17-19 June 1997.

[35] C. Xu and J. L. Prince. Snakes, shapes, and gradient vector flow. *IEEE Transactions on Image Processing*, 7(3), 1998.

[36] J. Sattar. Snakes, shapes and gradient vector flow. School of Computer Science, McGill University.

[37] Rafael C. Gonzalez and Richard E. Woods. *Digital Image Processing*. Addison-Wesley Longman Publishing Co., Inc., Boston, MA, USA, 2001.

[38] Chunming Li, Jundong Liu, and M.D. Fox. Segmentation of edge preserving gradient vector flow: an approach toward automatically initializing and splitting of snakes. In *Computer Vision and Pattern Recognition, 2005. CVPR 2005. IEEE Computer Society Conference on*, volume 1, pages 162–167vol.1, 20-25 June 2005.

[39] R. Pichuman. Snakes: an active model. http://homepages.inf.ed.ac.uk/rbf/CVonline/LOCAL_COPIES/RAMANI1/node31.html, [June 20, 2007].

[40] National Institute of Standards and Technology. Levenshtein distance. http://www.nist.gov/dads/HTML/Levenshtein.html, June 11, 2007 [June 20, 2007].

[41] L. Allison. Dynamic programming algorithm (dpa) for edit-distance. Monash University. http://www.csse.monash.edu.au/∼lloyd/tildeAlgDS/Dynamic/Edit/, 1999 [June 20, 2007].

[42] William K. Pratt. *Digital Image Processing: PIKS Inside*. John Wiley & Sons, Inc., New York, NY, USA, 2001.

Abbreviations

ABFO	American Board of Forensic Odontology
ADIS	Automated Dental Identification System
AFIS	Automated Fingerprint Identification System
AM	Ante-Mortem
AUC	Area Under the ROC Curve
CJIS	Criminal Justice Information Services Division
CNR	Contrast Noise Ratio
DC	Dental Code
DIR	Digital Image Repository
DNA	Deoxyribonucleic Acid
DR	Dental Radiograph
DTF	Dental Task Force
DW	Dental Work
DWM	Dental Works Mask
EER	Equal Error Rate
FAR	False Acceptance Rate
FRR	False Rejection Rate
FMR	False Match Rate
FNMR	False Non-Match Rate
FTA	Failure To Acquire
FTE	Failure To Enroll
GVF	Gradient Vector Flow
HMM	Hidden Markov Model
LED	Light Emitting Diode
LD	Levenshtein Distance
MUP	Missing and Unidentified Persons
NCIC	National Crime Information Center's
PCNN	Pulse Coupled Neural Network
PM	Post-Mortem
ROC	Receiver Operating Characteristic
ROI	Region Of Interest
SVM	Support Vector Machines
UNS	Universal Numbering System

Declaration of Sources and Access

I, the undersigned, the author of this thesis, declare that this thesis is my own work and has not been submitted in any form for another degree or diploma at any university or other institution of tertiary education. Information derived from the published or unpublished work of others has been acknowledged in the text and a list of references is provided.

I declare and understand that the Carinthia University of Applied Sciences / FH Technikum Kärnten will make my thesis available for use within the university library. I have been informed that the Carinthia Tech Institute is not liable for the misuse of its contents by third parties resulting from its reading. In particular, I have been informed that I am responsible for the registration of patents, trademarks or registered designs as well as any resulting claims.

Place, Date Sign